

Changepoint Detection in Complex Models: Cross-Fitting Is Needed

Chengde Qian^a, Guanghui Wang^b, Zhaojun Wang^b, and Changliang Zou^b

^a*School of Mathematical Sciences, Shanghai Jiao Tong University*

^b*School of Statistics and Data Science, Nankai University*

Abstract

Changepoint detection is commonly approached by minimizing the sum of in-sample losses to quantify the model’s overall fit across distinct data segments. However, we observe that flexible modeling techniques, particularly those involving hyperparameter tuning or model selection, often lead to inaccurate changepoint estimation due to biases that distort the target of in-sample loss minimization. To mitigate this issue, we propose a novel cross-fitting methodology that incorporates out-of-sample loss evaluations using independent samples separate from those used for model fitting. This approach ensures consistent changepoint estimation, contingent solely upon the models’ predictive accuracy across nearly homogeneous data segments. Extensive numerical experiments demonstrate that our proposed cross-fitting strategy significantly enhances the reliability and adaptability of changepoint detection in complex scenarios.

Keywords: Cross-fitting; Cross-validation; High-dimensional models; Model selection; Multiple changepoints; Predictive accuracy

1 Introduction

In modern big data analytics, datasets often exhibit shifts in distributions over time or space. Consider a sequence of observations $\{z_i\}_{i=1}^n$, where each z_i takes value in \mathcal{Z} and has a

distribution P_i . Our interest lies in detecting changes in parameters $f_i = f_i(P_i)$, which may be high- or infinite-dimensional. We focus on the following multiple changepoints model:

$$f_i = f_k^*, \quad i \in (\tau_{k-1}^*, \tau_k^*], \quad k = 1, \dots, K^* + 1; \quad i = 1, \dots, n, \quad (1)$$

where $\{\tau_k^*\}_{k=1}^{K^*}$ are the K^* changepoints that divide the data into $K^* + 1$ contiguous segments, each sharing a common parameter f_k^* , with the conventions $\tau_0^* = 0$ and $\tau_{K^*+1}^* = n$.

Changepoint detection aims to identify the true segmentation $\mathcal{T}^* = (\tau_1^*, \dots, \tau_{K^*}^*)$. This typically involves minimizing the sum of *in-sample losses* to quantify the model's overall fit across all data segments (Harchaoui and Lévy-Leduc, 2010; Aue and Lee, 2011; Killick et al., 2012; Zou et al., 2014). Define a potential segmentation as $\mathcal{T} = (\tau_1, \dots, \tau_K)$, comprising K ordered integers $\{\tau_k\}_{k=1}^K$ (with $\tau_0 = 0$ and $\tau_{K+1} = n$), and denote its cardinality by $|\mathcal{T}|$. The *total* in-sample loss is:

$$\mathcal{L}_{n,\text{in}}(\mathcal{T}) = \sum_{k=1}^{K+1} \mathcal{L}(z_{(\tau_{k-1}, \tau_k]}; \widehat{f}_{(\tau_{k-1}, \tau_k]}) + \gamma|\mathcal{T}|,$$

where for any index set $I \subset (0, n]$, $\mathcal{L}(z_I; f)$ evaluates the fit of the model with parameter f to the data segment $z_I = \{z_i : i \in I\}$, \widehat{f}_I denotes the parameter estimator for this segment, and $\gamma|\mathcal{T}|$ acts as a penalty to discourage over-segmentation, with $\gamma > 0$ being a prespecified parameter. If the true number of changepoints is known, one can set $\gamma = 0$ and $K = K^*$. Minimizing $\mathcal{L}_{n,\text{in}}(\mathcal{T})$ across all potential segmentations is often solved efficiently using dynamic programming techniques (Auger and Lawrence, 1989; Jackson et al., 2005; Killick et al., 2012). Approximate solutions can also be obtained through algorithms like binary segmentation (Fryzlewicz, 2014; Kovács et al., 2023) or moving windows (Hao et al., 2013; Eichinger and Kirch, 2018). For a comprehensive review, see Truong et al. (2020).

Traditional changepoint detection approaches typically employ models with finite-dimensional parameters, estimated through least squares or maximum likelihood technique (Csörgő and Horváth, 1997). A fundamental principle in this context is that the estimator \widehat{f}_I should uniformly approximate the target parameter (referred to as the *estimand*) $f_I^\circ = \arg \min_{f \in \mathcal{F}} \mathbb{E}\{\mathcal{L}(z_I; f)\}$ across all segments I , regardless of the presence of changepoints (Yao, 1988; Bai and Perron, 1998; Braun et al., 2000). Here \mathcal{F} denotes the set of all feasible parameters. This principle

of *uniform consistency* in parameter estimation is crucial for successful changepoint detection. Consider the total *oracle loss*—the population counterpart of the total in-sample loss $\mathcal{L}_{n,\text{in}}(\mathcal{T})$:

$$\bar{\mathcal{L}}^\circ(\mathcal{T}) = \sum_{k=1}^{K+1} \mathbb{E}\{\mathcal{L}(z_{(\tau_{k-1}, \tau_k]}; f_{(\tau_{k-1}, \tau_k]}^\circ)\} + \gamma|\mathcal{T}|,$$

which generally attains its minimum when $\mathcal{T} = \mathcal{T}^*$ (Londschien et al., 2023). For instance, consider detecting changes in the mean of a sequence of independent univariate normal data, where $\mathcal{Z} = \mathbb{R}$ and $P_i = \mathcal{N}(f_i, \sigma^2)$ with means f_i and a common variance σ^2 . A standard approach involves using the squared loss $\mathcal{L}(z_I; f) = \sum_{i \in I} (z_i - f)^2$. Accordingly, the estimand $f_I^\circ = \arg \min_{f \in \mathbb{R}} \mathbb{E}\{\sum_{i \in I} (z_i - f)^2\} = |I|^{-1} \sum_{i \in I} f_i$. The total oracle loss then becomes:

$$\bar{\mathcal{L}}^\circ(\mathcal{T}) = \sum_{k=1}^{K+1} \sum_{i \in (\tau_{k-1}, \tau_k]} (f_i - f_I^\circ)^2 + n\sigma^2 + \gamma|\mathcal{T}|,$$

which clearly reaches its minimum at $\mathcal{T} = \mathcal{T}^*$, with $f_i = f_k^*$ for all $i \in (\tau_{k-1}^*, \tau_k^*]$. In this setting, for any segment I , the sample average $|I|^{-1} \sum_{i \in I} z_i$ serves as \hat{f}_I , which minimizes $\mathcal{L}(z_I; f)$ over $f \in \mathbb{R}$. The uniform consistency of such \hat{f}_I to f_I° typically ensures that $\mathcal{L}_{n,\text{in}}(\mathcal{T})$ closely approximates $\bar{\mathcal{L}}^\circ(\mathcal{T})$, thereby allowing minimization of $\mathcal{L}_{n,\text{in}}(\mathcal{T})$ to yield solutions close to \mathcal{T}^* .

In modern contexts, changepoint models often encompass high- or infinite-dimensional parameters, complicating the fitting process. Table 1 showcases a list of complex changepoint models from recent research, where detection involves minimizing the total in-sample loss $\mathcal{L}_{n,\text{in}}(\mathcal{T})$, on either a global or local scale. Examples include linear regression (Lee et al., 2016; Leonardi and Bühlmann, 2016; Kaul et al., 2019; Rinaldo et al., 2021; Wang et al., 2021; Xu et al., 2024), quantile regression (Lee et al., 2018; Wang et al., 2024), Gaussian graphical models (Londschien et al., 2021; Liu et al., 2021), vector autoregression (Bai et al., 2023), trace regression (Shi et al., 2024), and nonparametric models (Arlot et al., 2019; Londschien et al., 2023). These detection approaches integrate advanced model fitting techniques such as lasso, random forests, and kernel methods. In many cases, the principle of uniform consistency remains relevant, ensuring consistent changepoint estimation. For example, in high-dimensional linear models with changepoints, the lasso estimator, equipped with

Table 1: Changepoint detection for complex models via minimizing the total in-sample loss.

$z_i \in \mathcal{Z}$	f_i	$\mathcal{L}(z_I; f)$	\hat{f}_I
<u>High-dimensional models</u>			
$z_i = (y_i, x_i) \in \mathbb{R} \times \mathbb{R}^p$	$\mathbb{E}(y_i x_i) = x_i^\top f_i$	$\sum_{i \in I} (y_i - x_i^\top f)^2$	$\hat{f}_I^{\text{lasso}\P}$
	$F_{y_i x_i}^{-1}(\alpha) = x_i^\top f_i^\S$	$\sum_{i \in I} \rho_\alpha(y_i - x_i^\top f)^\S\S$	\hat{f}_I^{lasso}
$z_i \in \mathbb{R}^p$	$f_i = (\mu_i, \Omega_i),$ $P_i = \mathcal{N}(\mu_i, \Omega_i^{-1})$	$ I \{ \text{tr}(\Omega^\top S_I) - \log \Omega \},$ $S_I = \sum_{i \in I} (z_i - \mu)(z_i - \mu)^\top, (I ^{-1} \sum_{i \in I} z_i, \hat{\Omega}_I^{\text{glasso}})$ $f = (\mu, \Omega)$	
$z_i \in \mathbb{R}^{p_1 \times p_2}$	$f_i = (L_i, S_i),$ $z_i \sim \mathcal{N}((L_i + S_i)z_{i-1}, \sigma^2 I)$ (Low-rank L_i , sparse S_i)	$\sum_{i \in I} \ z_i - (L + S)z_{i-1}\ ^2,$ $f = (L, S)$	$(\hat{L}_I^{\text{nuc}}, \hat{S}_I^{\text{lasso}})$
<u>Nonparametric models</u>			
General objects	$f_i = dP_i/d(n^{-1} \sum_{j=1}^n P_j)$	$-\sum_{i \in I} \log f(z_i)$	$\hat{f}_I(\cdot)^\dagger$
	$\int k_\gamma(z_i, \cdot) dP_i^\ddagger$	$\sum_{i \in I} \ k_\gamma(z_i, \cdot) - f\ _{\mathcal{H}_\gamma}^2$	$ I ^{-1} \sum_{j \in I} k_\gamma(z_j, \cdot)$

^{\P} The superscripts lasso/glasso (nuc) generally refer to L_1 - (nuclear-)norm regularized estimators, varying from context to context.

^{\S} For $\alpha \in (0, 1)$, $F_{y|x}^{-1}(\alpha)$ denotes the α -quantile of the conditional distribution $F_{y|x}$ of y given x .

^{\S\S} $\rho_\alpha(u) = u(\alpha - 1_{\{u < 0\}})$ is the quantile loss function.

^{\dagger} $\hat{f}_I(z_i)$ denotes the predicted class-1 probability for z_i , scaled by $n|I|^{-1}$, with the classifier trained based on inputs $\{z_i\}_{i=1}^n$ and artificially generated labels 1 for $i \in I$ and 0 otherwise; refer to Section 4.2.

^{\ddagger} $k_\gamma(\cdot, \cdot)$ denotes the kernel in a reproducing kernel Hilbert space, with a tuning hyperparameter γ .

an appropriately prespecified regularizer, uniformly approximates its population counterpart across different segments (Xu et al., 2024; Qian et al., 2023). Likewise, in other models, the estimated parameters \hat{f}_I can closely mirror their estimands f_I° , with suitable regularizers (Liu

et al., 2021; Bai et al., 2023; Wang et al., 2024) or kernels (Garreau and Arlot, 2018).

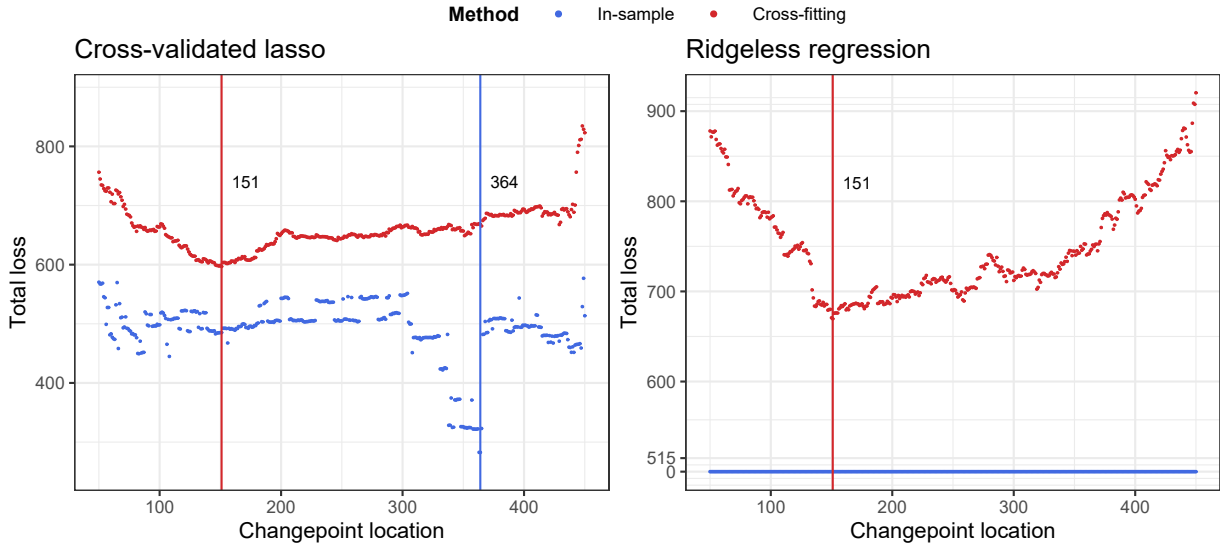


Figure 1: Curve of the total in-sample and out-of-sample losses plotted against the changepoint location, for cross-validated lasso and ridgeless regression in high-dimensional linear models (see Section 3). Specific model settings are provided in Section 4.1.1 and Section S.5 in Supplementary Material, with the true changepoint located at 150.

However, we observe that the utilization of flexible statistical and machine learning approaches frequently results in inaccurate changepoint detection. An illustrative example involves overparameterized deep neural networks, which typically achieve (near) perfect fits to training data—a phenomenon known as *interpolation* (Zhang et al., 2021; Belkin et al., 2019). Consequently, $\mathcal{L}(z_I; \hat{f}_I) \approx 0$ for any segment I , and $\mathcal{L}_{n,\text{in}}(\mathcal{T}) \approx 0$ for all segmentations \mathcal{T} , rendering accurate changepoint detection infeasible. Another instance occurs with high-dimensional linear models using cross-validated lasso estimators. Figure 1a depicts the curve of the total in-sample loss plotted against the changepoint location, which often attains a minimum far from the true changepoint. In these examples, the uniform consistency of \hat{f}_I relies on stringent model assumptions that may not hold in practice, leading the total in-sample loss $\mathcal{L}_{n,\text{in}}(\mathcal{T})$ to deviate significantly from the total oracle loss $\bar{\mathcal{L}}^\circ(\mathcal{T})$. This discrepancy results in unreliable changepoint estimators. For a formal theoretical justification, refer to Section 2.3.

Despite these challenges, modern machine learning techniques, such as random forest, kernel methods, and neural networks, are capable of capturing intricate data distributions and model architectures, offering significant potential for enhancing changepoint detection. Techniques like cross-validation facilitate the practical and automatic implementation of diverse learning procedures, improving the robustness and reproducibility in changepoint detection. How can these highly adaptive modeling approaches be safely employed for changepoint detection, and what underpins their effectiveness?

1.1 Our contributions

In essence, popular in-sample loss minimization methods succeed in changepoint detection by closely approximating the oracle losses $\mathbb{E}\{\mathcal{L}(z_I; f_I^\circ)\}$ for all segments I , thus aligning with the oracle minimization target $\bar{\mathcal{L}}^\circ(\mathcal{T})$. However, they may fall short for models prone to overfitting. Our approach introduces a simple yet effective remedy: *out-of-sample* loss evaluations. These evaluations are designed to estimate population losses using samples independent of those employed for model fitting, thereby producing unbiased estimators of expected losses conditional on model fits. We employ a *cross-fitting* strategy to facilitate efficient data reuse. As depicted in Figure 1, the total out-of-sample loss curve attains its minimum near the actual changepoint for both the cross-validated lasso and ridgeless regression approaches. Our contributions are twofold:

- We propose a cross-fitting method adaptable to various changepoint models, where detection relies on loss minimization. The minimization of total out-of-sample loss is easy to implement by incorporating diverse changepoint search algorithms, on either a global or local scale.
- We delineate the high-level prerequisites necessary for approximating oracle losses via empirical evaluations, ensuring consistent changepoint detection. Notably, cross-fitting alleviates some of these prerequisites, requiring only that models yield accurate predictions on nearly homogeneous data segments.

We further apply the proposed methodology and theoretical framework to the high-

dimensional linear models with changepoints, a topic of considerable interest, to demonstrate the practical relevance of our theoretical conditions and findings.

1.2 Related literature

Cross-fitting: Recently, cross-fitting has gained popularity as a method to enhance the efficiency and robustness of sample-splitting-based statistical inference. This approach relaxes the requirements imposed on estimation algorithms, allowing for the utilization of flexible machine learning techniques. It has been widely adopted in various domains, such as double machine learning (Chernozhukov et al., 2018), prediction-powered inference (Zhang and Bradic, 2022; Zrnic and Candès, 2024), and variable importance measurement (Williamson et al., 2023).

Out-of-sample evaluations: Londschien et al. (2023) explored detecting changes in nonparametric distributions, utilizing classifier log-likelihood ratios. The authors advocated for using random forests as classifiers, noting one of their attractive attributes: the ability to generate unbiased probability estimates through out-of-bag predictions. By incorporating binary segmentation search algorithm, they demonstrated consistent changepoint detection in scenarios with a single changepoint, relying on the uniform consistency assumption for the classifier. The out-of-bag mechanism inherent in random forests naturally provides an out-of-sample evaluation, similar to the approach we adopt here. In our manuscript, we systematically motivate the need and advantages of out-of-sample loss evaluations, addressing a critical gap between loss evaluation and changepoint detection in a more comprehensive framework encompassing multiple changepoints with flexible learning techniques beyond random forest classifiers. Additionally, we argue that the assumption of uniformly consistent model fits across all segments is excessively stringent.

1.3 Structure and notations

The remainder of this paper is structured as follows. Section 2 presents a general methodology and theoretical framework for changepoint detection via cross-fitting. Section 3 explores this approach within the context of high-dimensional linear models with changepoints. Simu-

lation studies and real-data analyses are detailed in Section 4. Section 5 concludes the paper. All theoretical proofs are provided in Supplementary Material.

For a positive integer n , let $[n] = \{1, \dots, n\}$. For $a, b \in \mathbb{R}$, $a \vee b = \max\{a, b\}$. For a vector $a \in \mathbb{R}^p$ and $q \in \{1, 2\}$, the L_q -norm of a is defined by $\|a\|_q = (\sum_{j=1}^p |a_j|^q)^{1/q}$, and let $\|a\| = \|a\|_2$. For a matrix $A \in \mathbb{R}^{p \times p}$, define $\|a\|_A = \sqrt{a^\top A a}$. For a matrix $A \in \mathbb{R}^{p_1 \times p_2}$, $A_{R,C}$ denotes the submatrix with rows indexed by R and columns indexed by C . Denote $A_R = A_{R,[p_2]}$ and $A_{R,-C} = A_{R,[p_2] \setminus C}$. For two sequences a_n and b_n , $a_n \asymp b_n$ if there exist constants c and C such that $c \leq |a_n/b_n| \leq C$ for sufficiently large n , $a_n \gg b_n$ means $a_n/b_n \rightarrow \infty$, and $a_n \gtrsim b_n$ means $a_n > Cb_n$ for a sufficiently large constant C or $a_n \gg b_n$. For a random variable X , define its sub-exponential norm as $\|X\|_{\Psi_1} = \inf\{t > 0 : \mathbb{E}\{\exp(|X|/t)\} \leq 2\}$, and its sub-Gaussian norm as $\|X\|_{\Psi_2} = \inf\{t > 0 : \mathbb{E}\{\exp(|X|^2/t)\} \leq 2\}$.

2 General framework

2.1 Changepoint detection via cross-fitting

Consider the multiple changepoints model (1). For a fixed integer $M \geq 2$, let $\{J_m\}_{m=1}^M$ be a partition of the index set $[n]$, such that $[n] = \cup_{m=1}^M J_m$ with disjoint subsets $J_m \subset [n]$. In contrast to minimizing the total in-sample loss $\mathcal{L}_{n,\text{in}}(\mathcal{T})$, our objective shifts to minimizing the total out-of-sample loss with a cross-fitting strategy:

$$\mathcal{L}_{n,\text{cf}}(\mathcal{T}) = \sum_{k=1}^{K+1} \sum_{m=1}^M \mathcal{L}(z_{(\tau_{k-1}, \tau_k] \cap J_m}; \hat{f}_{(\tau_{k-1}, \tau_k] \setminus J_m}) + \gamma |\mathcal{T}|,$$

where, for any segment $I \subset (0, n]$, $\hat{f}_{I \setminus J_m}$ represents the parameter estimator from the data excluding those in segment J_m . The model fitting procedure leading to $\hat{f}_{I \setminus J_m}$ can incorporate a variety of hyperparameter tuning and model selection techniques, such as feature screening, the use of information criteria, and cross-validation.

Remark 1 (On partitioning). To preserve the integral structure of changepoints, an order-preserving splitting method is recommended (Zou et al., 2020). Specifically, we set $J_m = \{i \in [n] : (i-1) \bmod M = m-1\}$ for each $m \in [M]$. In practice, we suggest $M = 5$ or 10 , aligning with common practices in cross-validation and cross-fitting techniques.

Let $\mathbb{T}(d_m)$ be the collection of all potential segmentations $\mathcal{T} = (\tau_1, \dots, \tau_K)$ such that the minimal segment length satisfies $\min_{k \in [K^*+1]} \{\tau_k - \tau_{k-1}\} \geq d_m$, where $d_m > 0$ is a prespecified integer. The changepoints are identified as

$$(\widehat{\tau}_{\text{cf},1}, \dots, \widehat{\tau}_{\text{cf},\widehat{K}_{\text{cf}}}) = \arg \min_{\mathcal{T} \in \mathbb{T}(d_m)} \mathcal{L}_{n,\text{cf}}(\mathcal{T}).$$

This minimization can be approached either globally or locally, employing search algorithms originally developed for optimizing the total in-sample loss $\mathcal{L}_{n,\text{in}}(\mathcal{T})$; refer to Section 1. Additionally, to expedite this search process, advanced techniques such as seeded intervals (Kovács et al., 2023), relief intervals (Qian et al., 2023), and optimistic search strategies (Kovács et al., 2020) can be incorporated.

Remark 2 (On cross-fitting and cross-validation recycles). Consider a model fitting procedure that entails hyperparameter tuning or model selection among a pool of candidates for each segment I : $\{\widehat{f}_I(\lambda) : \lambda \in \Lambda\}$. Cross-validation typically requires further partitioning I into B disjoint folds, say, $I = \cup_{b=1}^B V_{I,b}$, and the cross-validated model is defined as $\widehat{f}_I(\widehat{\lambda}_I^{\text{cv}})$, where

$$\widehat{\lambda}_I^{\text{cv}} \in \arg \min_{\lambda \in \Lambda} \sum_{b=1}^B \mathcal{L}(z_{V_{I,b}}; \widehat{f}_{I \setminus V_{I,b}}(\lambda)). \quad (2)$$

The cross-fitting strategy, paired with this cross-validation, necessitates running $MB|\Lambda|$ model fits for each segment I : $\{\widehat{f}_{(I \setminus J_m) \setminus V_{I \setminus J_m,b}}(\lambda) : m \in [M], b \in [B], \lambda \in \Lambda\}$. To optimize the use of “validation” datasets in both cross-fitting and cross-validation processes, we suggest a modified cross-validation strategy that seamlessly integrates with the cross-fitting scheme. Specifically, we set $B = M$ and $V_{I,m} = I \cap J_m$ for $m \in [M]$ for each I . This alignment enables the use of *recycled* out-of-sample losses:

$$\mathcal{L}_{\text{recyc},I} = \min_{\lambda \in \Lambda} \sum_{m=1}^M \mathcal{L}(z_{I \cap J_m}; \widehat{f}_{I \setminus J_m}(\lambda)),$$

effectively reducing the number of model fits required for each segment I to $M|\Lambda|$. The final total out-of-sample loss then becomes $\sum_{k=1}^{K+1} \mathcal{L}_{\text{recyc},(\tau_{k-1}, \tau_k]} + \gamma|\mathcal{T}|$.

2.2 Cross-fitting ensures consistent detection

For clarity, we introduce several notations related to different loss metrics within our framework. Consider a fixed model parameter f . At the individual level, denote the empirical

loss for data point z_i as $\ell(z_i; f)$, which quantifies the model's fit to z_i . The corresponding expected loss is $\bar{\ell}_i(f) = \mathbb{E}_{z_i}\{\ell(z_i; f)\}$. The *oracle* model parameter (or estimand) is defined as $f_i^\circ = \arg \min_{f \in \mathcal{F}} \bar{\ell}_i(f)$. Typically, the loss function ℓ is specified such that $f_i^\circ = f_k^*$ for $i \in (\tau_{k-1}^*, \tau_k^*]$. In the context of linear models with changepoints (refer to Section 3), the loss function is often chosen as the squared loss $\ell(z_i; f) = (y_i - x_i^\top f)^2$, and thus $\bar{\ell}_i(f) = \|f_i - f\|_\Sigma^2 + \sigma_\epsilon^2$, minimized at $f = f_i = f_k^*$ for $i \in (\tau_{k-1}^*, \tau_k^*]$ over $\mathcal{F} = \mathbb{R}$. Similarly, at the segment level, for any segment I , define the empirical loss as $\mathcal{L}(z_I; f) = \sum_{i \in I} \ell(z_i; f)$, and the expected loss as $\bar{\mathcal{L}}_I(f) = \mathbb{E}_{z_I}\{\mathcal{L}(z_I; f)\} = \sum_{i \in I} \bar{\ell}_i(f)$. The oracle parameter for segment I is identified as $f_I^\circ = \arg \min_{f \in \mathcal{F}} \bar{\mathcal{L}}_I(f)$. To quantify the signal of change at the changepoint τ_k^* for $k \in [K^*]$, we introduce

$$\Delta_k = \{\bar{\ell}_{\tau_k^*}(f_{k+1}^*) - \bar{\ell}_{\tau_k^*}(f_k^*)\} \vee \{\bar{\ell}_{\tau_k^*+1}(f_k^*) - \bar{\ell}_{\tau_k^*+1}(f_{k+1}^*)\},$$

with the conventions $\Delta_0 = \Delta_{K^*+1} = 0$. For linear models with squared loss, this metric simplifies to $\Delta_k = \|f_k^* - f_{k+1}^*\|_\Sigma^2$.

Condition 1 (Tails of the loss). For each $i \in [n]$, the random variable $s_{i,f} = \{\ell(z_i; f) - \ell(z_i; f_i^\circ)\} - \{\bar{\ell}_i(f) - \bar{\ell}_i(f_i^\circ)\}$ is bounded in the sub-exponential norm. Specifically, $\|s_{i,f}\|_{\Psi_1} \lesssim \{\bar{\ell}_i(f) - \bar{\ell}_i(f_i^\circ)\}^{1/2} \vee \{\bar{\ell}_i(f) - \bar{\ell}_i(f_i^\circ)\}$.

Condition 1 is essential for establishing nonasymptotic concentration inequalities related to empirical losses. For linear models with squared loss, $s_{i,f} = \{x_i^\top (f - f_i^\circ)\}^2 - \mathbb{E}[\{x_i^\top (f - f_i^\circ)\}^2] - 2\epsilon_i \{x_i^\top (f - f_i^\circ)\}$, which readily satisfies Condition 1 assuming that both the covariates x_i and the noise ϵ_i are sub-Gaussian (Vershynin, 2018). Additionally, other loss functions that exhibit Lipschitz continuity, such as quantile loss or Huber loss, are compatible with this condition.

Condition 2 (Model's predictive accuracy). There exists a positive constant \tilde{C} and a sequence of positive constants $d_{\text{acc},n} \gtrsim \log n$ such that, with probability at least $1 - \alpha_n$ (where $\alpha_n \rightarrow 0$), uniformly across each $m \in [M]$ and $I \in \mathcal{I}^{\text{nhomo}}$, $|\bar{\mathcal{L}}_{I \cap J_m}(\hat{f}_{I \setminus J_m}) - \bar{\mathcal{L}}_{I \cap J_m}(f_I^\circ)| \lesssim d_{\text{acc},n}$, where

$$\mathcal{I}^{\text{nhomo}} = \{(s, e) : |s - \tau_{k-1}^*| \leq \tilde{C} d_{\text{acc},n} \Delta_{k-1}^{-1}, |e - \tau_k^*| \leq \tilde{C} d_{\text{acc},n} \Delta_k^{-1}, \text{ for some } k \in [K^* + 1]\}.$$

Condition 2 underscores that the model fitting procedure should predict accurately on *nearly homogeneous* data segments identified within $\mathcal{I}^{\text{nhomo}}$. These segments include intervals where each endpoint should be within a distance of $O(d_{\text{acc},n}\Delta_{k-1}^{-1})$ or $O(d_{\text{acc},n}\Delta_k^{-1})$ samples from a changepoint. Notably, for linear models with squared loss, this condition manifests as $\|\widehat{f}_{I \setminus J_m} - f_I^\circ\|_\Sigma^2 \lesssim d_{\text{acc},n}/|I|$, which relates to parameter estimation error bound in the L_2 -norm. For lasso fit with an appropriately prespecified regularizer, $d_{\text{acc},n} = s_n \log p$, where s_n denotes sparsity and p is the dimension of covariates; see, e.g., Kaul et al. (2019) and Xu et al. (2024). The rate varies depending on the model, inherently determining the precision of estimated changepoints.

Condition 3 (Changes). (a) There exists a sufficiently large constant C_{snr} such that for $k \in [K^* + 1]$, $\tau_k^* - \tau_{k-1}^* \geq C_{\text{snr}}d_{\text{acc},n}(\Delta_{k-1}^{-1} \vee 1 + \Delta_k^{-1} \vee 1)$; (b) $\sup_{k \in [K^*]} \Delta_k \lesssim d_{\text{acc},n}/\log n$; (c) There exists a constant C_Δ such that for $k \in [K^*]$, $\Delta_k \leq C_\Delta[\{\bar{\ell}_{\tau_k^*}(f_{\{\tau_k^*, \tau_k^*+1\}}^\circ) - \bar{\ell}_{\tau_k^*}(f_k^*)\} + \{\bar{\ell}_{\tau_{k+1}^*}(f_{\{\tau_k^*, \tau_{k+1}^*+1\}}^\circ) - \bar{\ell}_{\tau_{k+1}^*}(f_{k+1}^*)\}]$.

Condition 3(a) imposes a minimum distance requirement between two successive changepoints. Condition 3(b) caps the magnitude of change signals while allowing vanishing magnitudes. Condition 3(c) is a technical requirement ensuring $\bar{\ell}_{\tau_k^*}(f_{\{\tau_k^*, \tau_k^*+1\}}^\circ) - \bar{\ell}_{\tau_k^*}(f_k^*)$ (or $\bar{\ell}_{\tau_{k+1}^*}(f_{\{\tau_k^*, \tau_{k+1}^*+1\}}^\circ) - \bar{\ell}_{\tau_{k+1}^*}(f_{k+1}^*)$) is comparable to $\bar{\ell}_{\tau_k^*}(f_{k+1}^*) - \bar{\ell}_{\tau_k^*}(f_k^*)$ (or $\bar{\ell}_{\tau_{k+1}^*}(f_k^*) - \bar{\ell}_{\tau_{k+1}^*}(f_{k+1}^*)$, respectively). By the definition of f_I° , we have $\Delta_k \geq \{\bar{\ell}_{\tau_k^*}(f_{\{\tau_k^*, \tau_k^*+1\}}^\circ) - \bar{\ell}_{\tau_k^*}(f_k^*)\} + \{\bar{\ell}_{\tau_{k+1}^*}(f_{\{\tau_k^*, \tau_{k+1}^*+1\}}^\circ) - \bar{\ell}_{\tau_{k+1}^*}(f_{k+1}^*)\}$, there is a naive lower bound $C_\Delta \geq 1$. In the case of linear models with squared loss, $f_{\{\tau_k^*, \tau_k^*+1\}}^\circ = (f_k^* + f_{k+1}^*)/2$, and recalling that $\Delta_k = \|f_k^* - f_{k+1}^*\|_\Sigma^2$, Condition 3(c) is easily satisfied with $C_\Delta = 2$.

Theorem 1. *Assuming Conditions 1–3 are satisfied, and employing a complete search algorithm with $d_m = C_m d_{\text{acc},n}$ and $\gamma = C_\gamma d_{\text{acc},n}$ for some positive constants C_m and C_γ , then there exists a positive constant C such that, with probability at least $1 - \alpha_n - n^{-C}$,*

$$\widehat{K}_{\text{cf}} = K^* \text{ and } \max_{1 \leq k \leq K^*} \min_{1 \leq j \leq \widehat{K}_{\text{cf}}} |\tau_k^* - \widehat{\tau}_{\text{cf},j}| \leq \widetilde{C} d_{\text{acc},n} \Delta_k^{-1}.$$

Theorem 1 demonstrates that the cross-fitting method, when integrated with a complete search algorithm (Jackson et al., 2005; Killick et al., 2012), provides consistent estimation

on both the number and locations of changepoints, given that $d_{\text{acc},n}\Delta_k^{-1}/n \rightarrow 0$. In particular, for linear models using standard lasso fits, this approach achieves a detection rate that aligns with the near-optimal benchmarks established in existing literature; see Section 3 for detailed discussions. Unlike traditional methods that are built on in-sample loss minimization, which require verifying uniform parameter estimation consistency across all data segments—whether homogeneous or heterogeneous, our cross-fitting approach substantially mitigates these stringent requirements. Specifically, it necessitates only verifying the models’ predictive accuracy on *nearly homogeneous* data segments, concerning *prediction* error, as detailed in Condition 2; further theoretical comparisons are explored in Section 2.3. This methodological shift, embracing the principles of sample-splitting and cross-fitting, moves away from the constraints typically imposed on parameter estimation in in-sample frameworks. Our approach offers great possibilities for employing diverse, flexible model fitting procedures focused on achieving high predictive accuracy, enhancing changepoint detection capabilities. Similar themes have been discussed in Chernozhukov et al. (2018), Zhang and Bradic (2022), and Williamson et al. (2023), though in different contexts. We will use high-dimensional linear models as an example for detailed illustration, in Section 3.

2.3 Theoretical comparison of in-sample and out-of-sample losses

Traditional changepoint analysis predominantly focuses on achieving uniform parameter estimation consistency across various data segments—accurately recovering oracle models f_I° , regardless of the presence of changepoints. Such consistency typically ensures that the total in-sample loss $\mathcal{L}_{n,\text{in}}(\mathcal{T})$ closely approximates the total oracle loss $\bar{\mathcal{L}}^\circ(\mathcal{T})$. Consequently, minimizing $\mathcal{L}_{n,\text{in}}(\mathcal{T})$ tends to yield solutions that approach the actual segmentation \mathcal{T}^* , the minimizer of $\bar{\mathcal{L}}^\circ(\mathcal{T})$ (Londschien et al., 2023). This section offers a formal and precise justification, through a novel perspective that shifts the focus from replicating oracle models to a critical emphasis on approximating oracle losses $\bar{\mathcal{L}}_I(f_I^\circ)$.

Let \mathcal{L}_I denote a general empirical loss evaluated with any model parameter estimator, encompassing both the in-sample loss $\mathcal{L}(z_I; \hat{f}_I)$ and the cross-fitted out-of-sample loss

$\sum_{m=1}^M \mathcal{L}(z_{I \cap J_m}; \hat{f}_{I \setminus J_m})$. Changepoints can then be identified as:

$$(\hat{\tau}_1, \dots, \hat{\tau}_{\hat{K}}) = \arg \min_{\mathcal{T} \in \mathbb{T}(d_m)} \left\{ \sum_{k=1}^K \mathcal{L}_{(\tau_{k-1}, \tau_k]} + \gamma |\mathcal{T}| \right\}.$$

Lemma 1. *Assuming Condition 3 is satisfied, and employing a complete search algorithm with $d_m = C_m d_{\text{acc},n}$ and $\gamma = C_\gamma d_{\text{acc},n}$ for some positive constants C_m and C_γ , then*

$$\hat{K} = K^* \text{ and } \max_{1 \leq k \leq K^*} \min_{1 \leq j \leq \hat{K}} \Delta_k |\tau_k^* - \hat{\tau}_j| \leq \tilde{C} d_{\text{acc},n},$$

conditional on the event $\mathbb{G} = \mathbb{G}^{\text{nhomo}} \cap \mathbb{G}^{-\text{nhomo}}$, where

$$\begin{aligned} \mathbb{G}^{\text{nhomo}} &= \{ \text{for any } I \in \mathcal{I}^{\text{nhomo}}, |\xi_I(\mathcal{L}_I)| < C_{1.1} d_{\text{acc},n} \}, \\ \mathbb{G}^{-\text{nhomo}} &= \{ \text{for any } I \notin \mathcal{I}^{\text{nhomo}} \text{ such that } |I| \geq d_m, \\ &\quad \xi_I(\mathcal{L}_I) > -[C_{1.2} \{\bar{\mathcal{L}}_I(f_I^\circ) - \sum_{i \in I} \bar{\ell}_i(f_i^\circ)\}] \vee (C_{1.1} d_{\text{acc},n}) \}, \end{aligned}$$

for some constants $C_{1.1} > 0$ and $C_{1.2} \in (0, 1/(1 + 4C_\Delta))$, and the approximation error

$$\xi_I(\mathcal{L}_I) = \left\{ \mathcal{L}_I - \sum_{i \in I} \ell(z_i; f_i^\circ) \right\} - \left\{ \bar{\mathcal{L}}_I(f_I^\circ) - \sum_{i \in I} \bar{\ell}_i(f_i^\circ) \right\},$$

quantifies the discrepancy between the general empirical loss and the corresponding oracle loss, properly centered, for segment I . The constants C_γ and \tilde{C} depend only on $C_{1.1}$, $C_{1.2}$, C_m , C_{snr} and C_Δ . In addition, The constants C_γ and \tilde{C} depend only on $C_{1.1}$, $C_{1.2}$, C_m , C_{snr} and C_Δ .

Lemma 1 elucidates that consistent changepoint detection hinges on how closely empirical losses approximate oracle losses, as quantified by $\xi_I(\mathcal{L}_I)$, across different types of data segments. For the nearly homogeneous segments $\mathcal{I}^{\text{nhomo}}$, the approximation error is roughly required such that $|\xi_I(\mathcal{L}_I)| \lesssim d_{\text{acc},n}$, while for the rest segments, only a lower bound on the approximation error is needed.

When applying a specific changepoint model and model fitting procedure, it necessitates ensuring that the event \mathbb{G} holds with high probability. For in-sample loss minimization approaches, this is generally established with the help of the uniform control of model parameter estimation errors across all segments (Lee et al., 2016; Leonardi and Bühlmann, 2016; Xu

et al., 2024; Lee et al., 2018; Wang et al., 2024; Bai et al., 2023; Shi et al., 2024; Londschien et al., 2023). In contrast, out-of-sample loss evaluations (and cross-fitting) enable us to more readily demonstrate the validity of \mathbb{G} . For the part $\mathbb{G}^{-\text{nhomo}}$, it holds under less stringent conditions on the loss and the changepoint model, say Conditions 1 and 3. However, these conditions alone are often insufficient for in-sample loss minimization approaches, as the in-sample loss $\mathcal{L}(z_I; \widehat{f}_I)$ may be significantly biased downwards due to overfitting—see Section 3 for a concrete example. For the part $\mathbb{G}^{\text{nhomo}}$, it holds under additional Condition 2, which stipulates that models need only predict well on nearly homogeneous segments in terms of prediction error.

3 A concrete example: high-dimensional linear models

Theorem 1 outlines high-level prerequisites for the changepoint model, loss function, and model fitting procedure to ensure accurate changepoint detection via the proposed cross-fitting method. To elucidate the practical implications of these conditions and conclusions, this section applies the general framework to a specific example: high-dimensional linear models with changepoints. Consider pairs of response and covariates $z_i = (y_i, x_i) \in \mathbb{R} \times \mathbb{R}^p$, where $y_i = x_i^\top f_k^* + \epsilon_i$, with ϵ_i representing mean-zero noise. The objective is to detect changes in the regression coefficients f_k^* under scenarios where $p \gtrsim n$. This changepoint model has received significant attention in recent years, with notable contributions including Lee et al. (2016), Leonardi and Bühlmann (2016), Kaul et al. (2019), Rinaldo et al. (2021), Wang et al. (2021), and Xu et al. (2024). Condition 1' is similar to the common assumptions in the literature, ensuring that Condition 1 is satisfied.

Condition 1' (Linear model and loss). (a) The covariates x_i are i.i.d. sub-Gaussian with zero mean and covariance matrix Σ , and $\|\Sigma^{-1/2}x_i\|_{\Psi_2} \leq C_x$ for some constant $C_x > 0$; (b) The noises ϵ_i are i.i.d. sub-Gaussian with zero mean, variance σ_ϵ^2 , and $\|\epsilon_i\|_{\Psi_2} \leq C_\epsilon$ for some constant $C_\epsilon > 0$; (c) There exists a sequence of integers s_n such that $|\{j \in [p] : f_{k,j}^* \neq 0\}| \leq s_n < p$. In addition, $|f_{k,j}^*| \leq C_f$ for some constant $C_f > 0$; (d) The loss function $\ell(z_i; f)$ is taken as $(y_i - x_i^\top f)^2$.

To examine the impact of model overfitting on changepoint detection, particularly in high-dimensional settings, we explore three distinct model fitting procedures that utilize in-sample loss minimization. Let $y = (y_1, \dots, y_n)^\top$ and $X = (x_1^\top, \dots, x_n^\top)^\top$.

- **Least squares on selected variables:** This procedure involves selecting a set of potentially relevant variables, denoted as X_{I, \widehat{S}_I} , with an index subset $\widehat{S}_I \subset [p]$, and performing least squares regression on these selected variables. It yields the parameter estimator $\widehat{f}_I^{\text{ls}}$, with $\widehat{f}_{I, \widehat{S}_I}^{\text{ls}} = (X_{I, \widehat{S}_I}^\top X_{I, \widehat{S}_I})^{-1} X_{I, \widehat{S}_I}^\top y_I$ and $\widehat{f}_{I, -\widehat{S}_I}^{\text{ls}} = 0$.

- **Cross-validated lasso:** A lasso estimator with a prespecified regularizer λ is defined by:

$$\widehat{f}_I^{\text{lasso}}(\lambda) \in \arg \min_{f \in \mathbb{R}^p} \{ \mathcal{L}(z_I; f) + \lambda \sqrt{|I|} \|f\|_1 \}, \quad (3)$$

where $\mathcal{L}(z_I; f) = \|y_I - X_I f\|^2$. The optimal regularizer, $\widehat{\lambda}_I^{\text{cv}}$, is determined through standard cross-validation; see Eq. (2). The cross-validated lasso estimator is then defined as $\widehat{f}_I^{\text{lasso}}(\widehat{\lambda}_I^{\text{cv}})$.

- **Ridgeless regression:** The estimator is the minimum L_2 -norm least squares solution $\widehat{f}_I^{\text{rl}} = (X_I^\top X_I)^+ X_I^\top y_I$ (Bartlett et al., 2020; Hastie et al., 2022), where A^+ denotes the Moore-Penrose pseudoinverse of matrix A .

Ridgeless regression models interpolate the data such that $\mathcal{L}(z_I; \widehat{f}_I^{\text{rl}}) = 0$. Consequently, $\mathcal{L}_{n, \text{in}}(\mathcal{T}) = 0$ for all candidate segmentations \mathcal{T} , rendering them indistinguishable. To analyze the impact of model selection and hyperparameter tuning on the other two procedures, we introduce a formula that specifies the approximation error $\xi_I(\mathcal{L}_I)$, as in Lemma 1.

Proposition 1. *Under Condition 1', for $\widehat{f}_I \in \{\widehat{f}_I^{\text{ls}}, \widehat{f}_I^{\text{lasso}}(\lambda), \widehat{f}_I^{\text{lasso}}(\widehat{\lambda}_I^{\text{cv}})\}$,*

$$\xi_I(\mathcal{L}_I) = \underbrace{O_p\left(\sqrt{\sum_{i \in I} \|f_i^\circ - f_i^\circ\|_\Sigma^2} \cdot \sqrt{s_n \log n}\right)}_{\text{Concentration error}} \underbrace{-2 \underbrace{u_I^\top X_I (\widehat{f}_I - f_I^\circ)}_{\text{Cross}} + \underbrace{\|X_I (\widehat{f}_I - f_I^\circ)\|^2}_{\text{Squared}}}_{\text{Bias}},$$

where $u_I = y_I - X_I f_I^\circ$.

The concentration error quantifies the rate at which the empirical loss $\sum_{i \in I} \{(y_i - x_i^\top f_I^\circ)^2 - \epsilon_i^2\}$ converges to its expectation $\sum_{i \in I} \|f_i^\circ - f_i^\circ\|_\Sigma^2$. The bias measures the impact of evaluating

the in-sample loss at \hat{f}_I rather than at f_I° . According to Lemma 1, it is generally required that $|\xi_I(\mathcal{L}_I)| \lesssim d_{\text{acc},n}$ for nearly homogeneous segments and $\xi_I(\mathcal{L}_I) > -(C_{1.2} \sum_{i \in I} \|f_i^\circ - f_I^\circ\|_\Sigma^2) \vee (C_{1.1} d_{\text{acc},n})$ for the rest segments, to ensure that changepoints can be accurately detected within the precision $\Delta_k^{-1} d_{\text{acc},n}$.

If the bias is $O_p(s_n \log p)$ —for instance, when employing $\hat{f}_I^{\text{lasso}}(\lambda^\circ)$ with $\lambda^\circ \asymp \sqrt{\log p}$ (Lee et al., 2016; Leonardi and Bühlmann, 2016)—this detection precision is guaranteed with $d_{\text{acc},n} = s_n \log p$, aligning with nearly optimal detection rates (Rinaldo et al., 2021).

However, there are instances where the bias could become the dominating term, exceeding $s_n \log p$. For example, consider $\hat{f}_I = \hat{f}_I^{\text{ls}}$, assuming the sure screening property holds (Fan and Lv, 2008). The bias becomes $-u_I^\top X_{I, \hat{S}_I} (X_{I, \hat{S}_I}^\top X_{I, \hat{S}_I})^{-1} X_{I, \hat{S}_I}^\top u_I$. For a *given* homogeneous segment I , this bias = $O_p(|\hat{S}_I| \log p)$, as demonstrated by Fan et al. (2012) in the context of error variance estimation with high-dimensional covariates. Similarly, for a homogeneous segment I and $\hat{f}_I = \hat{f}_I^{\text{lasso}}(\hat{\lambda}_I^{\text{cv}})$ with an active set \hat{S}_I , bias = $O_p(\sqrt{(|\hat{S}_I| + s_n) s_n \log^{3/2} p})$, as noted in Chetverikov et al. (2021); refer to Table S1 in Supplemental Material. Consequently, when the number of selected variables $|\hat{S}_I|$ substantially exceeds s_n —perhaps due to a lenient screening rule or a small regularizer—the bias may dominate. This dominance can compromise the near-optimal detection rate, and a large change signal might be necessary to enable consistent changepoint detection, albeit at a reduced level of precision.

In contrast, employing cross-validated lasso fits within an out-of-sample loss evaluation framework—specifically, by using $\mathcal{L}_{I, \text{cf}} = \sum_{m=1}^M \mathcal{L}(z_{I \cap J_m}; \hat{f}_{I \setminus J_m}^{\text{lasso}}(\hat{\lambda}_{I \setminus J_m}^{\text{cv}}))$ —could generally ensure bias = $O_p(s_n \log^2 p)$, matching the ideal scenarios up to a logarithmic factor. Examining a parallel version of Proposition 1:

$$\begin{aligned} \xi_I(\mathcal{L}_{I, \text{cf}}) &= O_p\left(\sqrt{\sum_{i \in I} \|f_i^\circ - f_I^\circ\|_\Sigma^2} \cdot \sqrt{s_n \log n}\right) \\ &\quad - \underbrace{\sum_{m=1}^M \left\{ 2 u_{I \cap J_m}^\top X_{I \cap J_m} \left(\hat{f}_{I \setminus J_m}^{\text{lasso}}(\hat{\lambda}_{I \setminus J_m}^{\text{cv}}) - f_I^\circ \right) \right\}}_{\text{Cross}} + \underbrace{\sum_{m=1}^M \left\| X_{I \cap J_m} \left(\hat{f}_{I \setminus J_m}^{\text{lasso}}(\hat{\lambda}_{I \setminus J_m}^{\text{cv}}) - f_I^\circ \right) \right\|^2}_{\text{Squared}}. \end{aligned}$$

The cross term exhibits a mean of zero, due to the independence between $z_{I \cap J_m}$ and $\hat{f}_{I \setminus J_m}^{\text{lasso}}(\hat{\lambda}_{I \setminus J_m}^{\text{cv}})$, together with a variance of $O_p(s_n \log^2 p)$ (Chetverikov et al., 2021).

For a formal and precise justification, we present conditions and a corollary of Theorem 1, tailored for the high-dimensional linear models.

Condition 2'. (Predictive accuracy) There exists a positive constant C such that, with probability at least $1 - n^{-C}$, $\|\hat{f}_{I \setminus J_m}^{\text{lasso}}(\hat{\lambda}_{I \setminus J_m}^{\text{cv}}) - f_I^\circ\|_\Sigma^2 \lesssim s_n(\log^2 p)/|I|$ for each $m \in [M]$ and $I \in \mathcal{I}^{\text{nhomo}}$.

Condition 3' (Changes). There exists a sufficiently large constant C_{snr} such that for $k \in [K^* + 1]$, $\tau_k^* - \tau_{k-1}^* \geq C_{\text{snr}} s_n(\log^2 p)(\Delta_{k-1}^{-1} \vee 1 + \Delta_k^{-1} \vee 1)$.

Condition 2' requires that the cross-validated lasso accurately predicts within nearly homogeneous data segments uniformly. The squared L_2 -norm $\|\hat{f}_{I \setminus J_m}^{\text{lasso}}(\hat{\lambda}_{I \setminus J_m}^{\text{cv}}) - f_I^\circ\|_\Sigma^2$ aligns directly with the prediction error $|I|^{-1}\{\bar{\mathcal{L}}_{I \cap J_m}(\hat{f}_{I \setminus J_m}^{\text{lasso}}(\hat{\lambda}_{I \setminus J_m}^{\text{cv}})) - \bar{\mathcal{L}}_{I \cap J_m}(f_I^\circ)\}$. For a *given* homogeneous segment I , Chetverikov et al. (2021) shows that for any $\alpha \in (0, 1)$, $\|\hat{f}_{I \setminus J_m}^{\text{lasso}}(\hat{\lambda}_{I \setminus J_m}^{\text{cv}}) - f_I^\circ\|_\Sigma \lesssim \sqrt{s_n \log(p/\alpha)/|I|} \times \sqrt{\log(pn)}$ holds with probability at least $1 - \alpha - n^{-C}$. Selecting $\alpha = n^{-C}$ with $C > 2$ results in

$$\|\hat{f}_{I \setminus J_m}^{\text{lasso}}(\hat{\lambda}_{I \setminus J_m}^{\text{cv}}) - f_I^\circ\|_\Sigma \lesssim \sqrt{s_n(\log^2 p)/|I|},$$

uniformly across all homogeneous segments I . This prediction accuracy could be extended to the nearly homogeneous case $(\tau_{k-1}^*, \tau_k^* + t]$ or $(\tau_{k-1}^* - t, \tau_k^*]$ that slightly extends the homogeneous segment by t points with $t \lesssim d_{\text{acc},n}$.

Corollary 1. *Assuming Conditions 1'–3' are satisfied, and employing a complete search algorithm with $d_m = C_m d_{\text{acc},n}$ and $\gamma = C_\gamma d_{\text{acc},n}$ for some positive constants C_m and C_γ , then there exists a positive constant C such that, with probability at least $1 - n^{-C}$,*

$$\hat{K}_{\text{cf}} = K^* \text{ and } \max_{1 \leq k \leq K^*} \min_{1 \leq j \leq \hat{K}_{\text{cf}}} \Delta_k |\tau_k^* - \hat{\tau}_{\text{cf},j}| \leq \tilde{C} s_n \log^2 p.$$

Corollary 1 confirms the consistency of changepoint detection employing cross-validated lasso fits, highlighting that the detection rate is minimax optimal up to a logarithmic factor (Rinaldo et al., 2021). Previous studies demonstrated that an accuracy of order $s_n \log p$ can be achieved within in-sample loss minimization frameworks, notably when lasso regularizers are carefully prespecified (Lee et al., 2016; Leonardi and Bühlmann, 2016; Kaul et al., 2019;

Rinaldo et al., 2021; Wang et al., 2021; Xu et al., 2024). These results depend heavily on the verification of the uniform estimation consistency of lasso fits $\hat{f}_I^{\text{lasso}}(\lambda)$ with prespecified regularizers to oracle models f_I° . In contrast, our cross-fitting approach achieves comparable detection accuracy while providing flexibility in hyperparameter tuning, which adapts to the intrinsic smoothness and heterogeneity among different segments, as evidenced by our numerical studies.

Remark 3 (On ridgeless fits). The extension of consistency theories to include ridgeless fits is intriguing. For a given segment I without changepoints, Bartlett et al. (2020) demonstrates that the ridgeless estimator can achieve near-optimal prediction accuracy, specifically, $\|\hat{f}_I^{\text{rl}} - f_I^\circ\|_\Sigma$ can be well-bounded, provided that the covariance matrix Σ is *benign* (cf. Definition 4 in Bartlett et al. (2020)). Establishing a uniform bound similar to Condition 2' could ensure the predictive accuracy necessary for consistent changepoint detection.

4 Numerical studies

4.1 High-dimensional linear models with changepoints

This section evaluates the performance of out-of-sample loss evaluations and cross-fitting strategies in high-dimensional linear models with changepoints, as described in Section 3. We employ lasso model fitting procedures with various approaches to tuning parameter selection. To ensure a controlled comparison, we set $\hat{K} = K^*$ and use a dynamic programming algorithm for both in-sample and out-of-sample loss minimization. The accuracy of detected changepoints is measured using the Hausdorff distance:

$$\max \left\{ \max_{1 \leq j \leq \hat{K}} \min_{1 \leq k \leq K^*} |\tau_k^* - \hat{\tau}_j|, \max_{1 \leq k \leq K^*} \min_{1 \leq j \leq \hat{K}} |\tau_k^* - \hat{\tau}_j| \right\},$$

based on 500 replications.

In-sample benchmarks: Current in-sample loss minimization approaches commonly employ lasso fits $\hat{f}_I^{\text{lasso}}(\lambda)$ (cf. Eq. (3)) with a universal λ across all segments I . To identify a suitable λ value, a *hold-out* technique is often recommended (Leonardi and Bühlmann, 2016; Rinaldo et al., 2021; Xu et al., 2024). This technique involves firstly partitioning the

data into a training set and a hold-out set, consisting of odd- and even-indexed observations, respectively. Then, the in-sample loss minimization is conducted on the training set, exploring a range of λ values. Each λ induces a specific changepoint model, with a sequence of estimated changepoints and their associated segment-specific linear models. The efficacy of each model configuration, dictated by λ , is then assessed on the hold-out set using the mean squared prediction error. The λ that yields the lowest prediction error is selected as optimal. To maximize data utilization, we refit the final changepoint model to the entire dataset using this optimal λ . Alternatively, we utilize cross-validated lasso fits $\hat{f}_I^{\text{lasso}}(\hat{\lambda}_I^{\text{cv}})$, with $\hat{\lambda}_I^{\text{cv}}$ defined in Eq. (2) (with $B = M$). These two methods of in-sample loss minimization with tailored tuning parameters are referred to as **in-ho** and **in-cv**, respectively.

Cross-fitting implementations: The **in-ho** approach can be adapted to an out-of-sample setting by substituting in-sample losses $\mathcal{L}(z_I; \hat{f}_I^{\text{lasso}}(\lambda))$ with out-of-sample losses $\sum_{m=1}^M \mathcal{L}(z_{I \cap J_m}; \hat{f}_{I \setminus J_m}^{\text{lasso}}(\lambda))$. This method is termed as **cf-ho**. Similarly, **in-cv** has a direct cross-fitting counterpart, named **cf-cv**, by replacing $\mathcal{L}(z_I; \hat{f}_I^{\text{lasso}}(\hat{\lambda}_I^{\text{cv}}))$ with the cross-fitted loss $\sum_{m=1}^M \mathcal{L}(z_{I \cap J_m}; \hat{f}_{I \setminus J_m}^{\text{lasso}}(\hat{\lambda}_{I \setminus J_m}^{\text{cv}}))$. Additionally, a recycling scheme, as introduced in Remark 2, is also employed, which is referred to as **cf-cv***.

4.1.1 Tuning impacts

We examine the influence of the tuning parameter λ on changepoint detection accuracy, considering a scenario with $(n, p, K^*, \tau_1^*) = (500, 1000, 1, 150)$. The covariates x_i are i.i.d. from $\mathcal{N}(0, \Sigma)$ with $\Sigma_{ij} = 0.2^{|i-j|}$, and the noises ϵ_i are i.i.d. from $\mathcal{N}(0, 1)$. The regression coefficients change from $f_1^* = (1, -1, 1, -1, 1, 0, \dots, 0)^\top$ to $f_2^* = (1 + \sqrt{b/5})f_1^*$, with $b \in \{0.5, 1, 5\}$ to reflect changes ranging from mild to substantial. Here, $\mathbf{1}_s$ denotes a vector in \mathbb{R}^p with the first s entries being one and the rest being zero.

Figure 2 depicts the curve of the average of empirical Hausdorff distances plotted against $\log \lambda$, where smaller λ values indicate a tendency towards overfitting. It compares the performance of in-sample loss minimization and cross-fitting evaluations (with 5 or 10 folds). Consistently, the cross-fitting method either matches or surpasses the in-sample methods, particularly demonstrating superior performance in regimes prone to overfitting. Such supe-

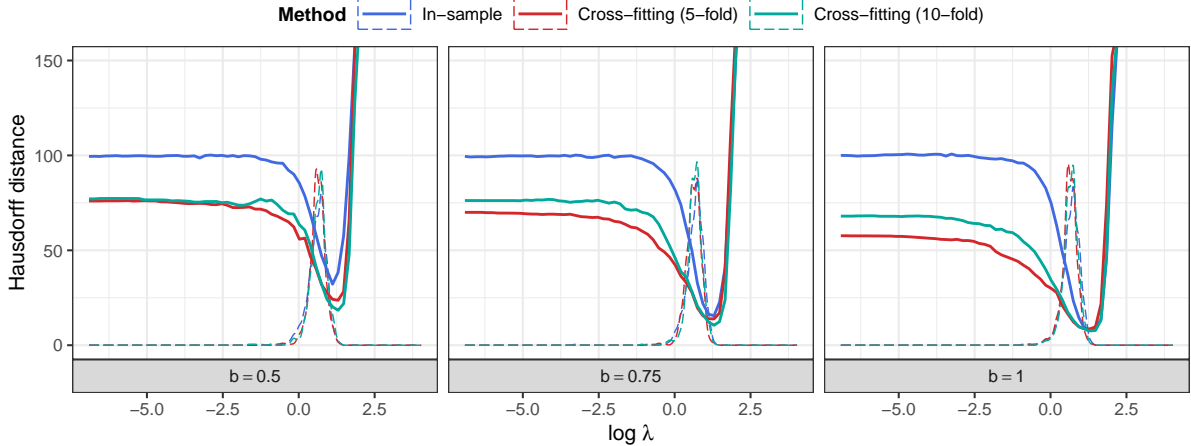


Figure 2: Influence of the tuning parameter on changepoint detection accuracy in high-dimensional linear models.

riority is more pronounced in scenarios with larger changes, where heavily overfitting lasso estimators, despite producing many false positives, can still predict well. This observation aligns with the insights from Proposition 1. Dotted curves in Figure 2 indicate the density of the tuning parameter selections made by **in-ho** and **cf-ho**, generally coinciding with more overfitting regions where cross-fitting outperforms. This suggests that out-of-sample strategies, utilizing a common data-driven tuning parameter, can provide more accurate changepoint estimation compared to in-sample implementations that use a similar tuning approach.

Figure 3 presents the boxplot of empirical Hausdorff distances, comparing various in-sample and cross-fitting methods that employ data-driven tuning parameter selections. Generally, the in-sample methods like **in-ho** and **in-cv** exhibit higher detection errors. In contrast, their out-of-sample counterparts, **cf-ho** and **cf-cv**, respectively, show a substantial reduction in these errors. In addition, the **cf-cv*** method, which utilizes a recycling scheme for validation, demonstrates comparable detection accuracy to the **cf-cv** method.

4.1.2 Segment-specific tuning or global tuning

We compare the efficacy of segment-specific tuning, where regularizers are determined individually for each segment (**cf-cv** and **cf-cv***), against global tuning, which utilizes

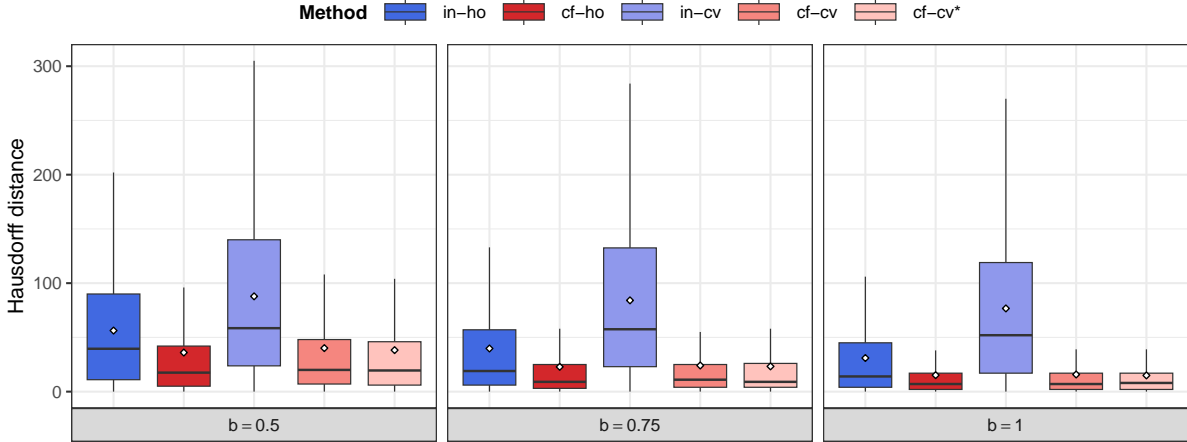


Figure 3: Boxplot of empirical Hausdorff distances for various in-sample and cross-fitting methods in high-dimensional linear models with a single changepoint.

a universal regularizer across all segments (**cf-ho**). This comparison is conducted under two distinct data generating processes (DGPs). Both setups involve a configuration of $(n, p, K^*) = (1000, 1000, 3)$, with $\{\tau_k^*\}_{k=1}^3 = \{350, 500, 880\}$. The covariates x_i are generated i.i.d. from $\mathcal{N}(0, \Sigma)$, where $\Sigma_{ij} = 0.2^{|i-j|}$.

- **DGP 1:** The regression coefficients are set as $f_1^* = f_3^* = (1, -1, 1, -1, 1, 0, \dots, 0)^\top$, $f_2^* = (1 + \sqrt{b/5})f_1^*$, and $f_4^* = (1 - \sqrt{b/5})f_1^*$, where b ranges over $\{0.6, 0.8, 1\}$ to simulate different levels of change signal strength. The noises ϵ_i are i.i.d. from $\mathcal{N}(0, 1)$.
- **DGP 2:** The regression coefficients are set as $f_1^* = f_3^* = \mathbf{1}_5$, $f_2^* = \mathbf{1}_5 + \mathbf{q}/\|\mathbf{q}\|_2$, and $f_4^* = \mathbf{1}_5 - 0.9\mathbf{q}/\|\mathbf{q}\|_2$, where $\mathbf{q} = (1, -1.3, 1, -1.3, 1, 0, \dots, 0)^\top$. The noises ϵ_i are Gaussian with zero mean, and their variances are adjusted to maintain a constant variance of the responses y_i across all segments, compensating for the variability introduced by changes in f_k^* . The minimum standard deviation of the noises, $se = \min_i \{\text{Var}(\epsilon_i)\}^{1/2}$, varies across $\{0.8, 0.5, 0.2\}$ to represent different levels of change signal strength.

Unlike DGP 1, DGP 2 introduces additional data heterogeneity through the variability in noise variance across segments. To expedite the search for multiple changepoints in high-dimensional settings, we incorporate the Reliever technique (Qian et al., 2023) into both in-sample and out-of-sample loss minimization.

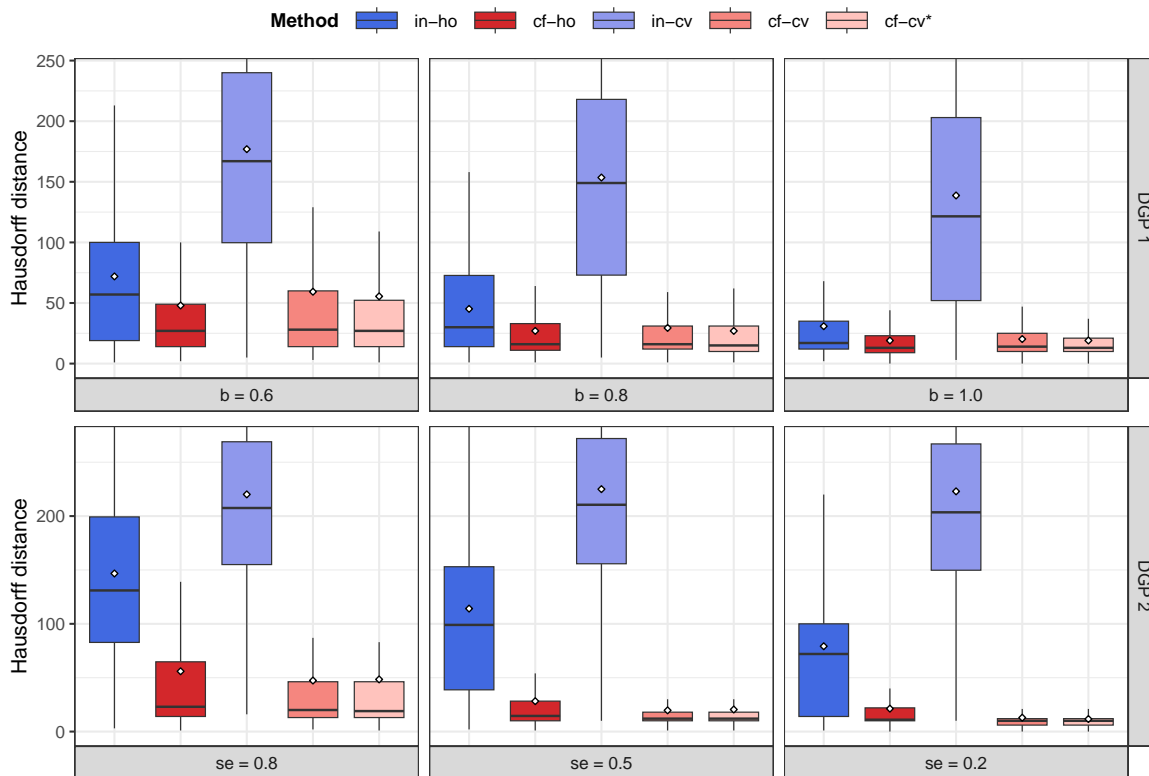


Figure 4: Boxplot of empirical Hausdorff distances for various in-sample and cross-fitting methods in high-dimensional linear models with multiple changepoints.

Figure 4 displays the boxplot of empirical Hausdorff distances for each tuning approach under both DGPs. We observe that cross-fitting-based methods consistently achieve reduced detection error compared to their in-sample counterparts across all DGP: **cf-ho** improves over **in-ho**, and **cf-cv** over **in-cv**. Additionally, **cf-cv*** delivers performance comparable to **cf-cv**. Moreover, under DGP 1, the segment-specific tuning approach **cf-cv** exhibits detection accuracy comparable to the global tuning approach **cf-ho** on average, while under DGP 2, **cf-cv** achieves uniformly lower detection error than **cf-ho**, highlighting the advantages of segment-specific tuning in settings with increased heterogeneity.

4.2 Nonparametric changepoint detection via classifiers

This section explores detecting distributional changes under Model (1), where $f_i = P_i$, or in a reparameterized form, $f_i = dP_i/d(n^{-1} \sum_{j=1}^n P_j)$ —the likelihood ratios. Lonschien et al. (2023) proposed a nonparametric framework for changepoint detection via probabilistic classifiers. This method falls within the in-sample loss minimization framework, where the loss function for any segment I is defined as $\mathcal{L}(z_I; f) = -\sum_{i \in I} \log f(z_i)$, with a functional parameter $f : \mathcal{Z} \rightarrow \mathbb{R}$. To enable dynamic programming-based minimization, we slightly modify the classifier-based parameter estimation procedure by employing a binary $\{0, 1\}$ -labeling system. Specifically, for each segment I , we first label data points within I as 1 and those outside I as 0, and then train a classifier using these binary labels along with all input data $\{z_i\}_{i=1}^n$. The proposed estimator is $\hat{f}_I(z) = n|I|^{-1}\hat{p}_I(z)$, where the trained classifier outputs $\hat{p}_I(z)$, representing the estimated probability that a given data point z is predicted as class 1.

For probabilistic classifiers, we consider:

- **Random forest**, implemented in the R package `ranger`, exploring the number of trees in $\{25, 50, 100\}$ and the minimum node size in $\{5, 10, 15\}$.
- **Gradient boosting**, implemented in `lightgbm`, setting the number of training rounds in $\{5, 15, 25\}$, the minimum gain to split in $\{0.1, 0.5\}$, and the learning rate in $\{0.05, 0.1\}$.
- **Multi-layer perceptron (MLP)**, with depth 3, width 128, and a logistic output layer, implemented in `torch`, utilizing the SGD optimizer with a batch size of 50 and the learning rate in $\{0.01, 0.1, 1\}$.

Each combination of candidate hyperparameters is evaluated using hold-out or cross-validation strategies, as discussed in Section 4.1. To expedite the changepoint search process with these complex fitting procedures, we again integrate the Reliever technique (Qian et al., 2023) into the dynamic programming algorithm. Out-of-sample loss evaluations are conducted following the framework described in Section 2.1. We implement several changepoint detection approaches: **in-ho**, **in-cv**, **cf-ho**, and **cf-cv*** (where the recycling version is used to ease computational burdens).

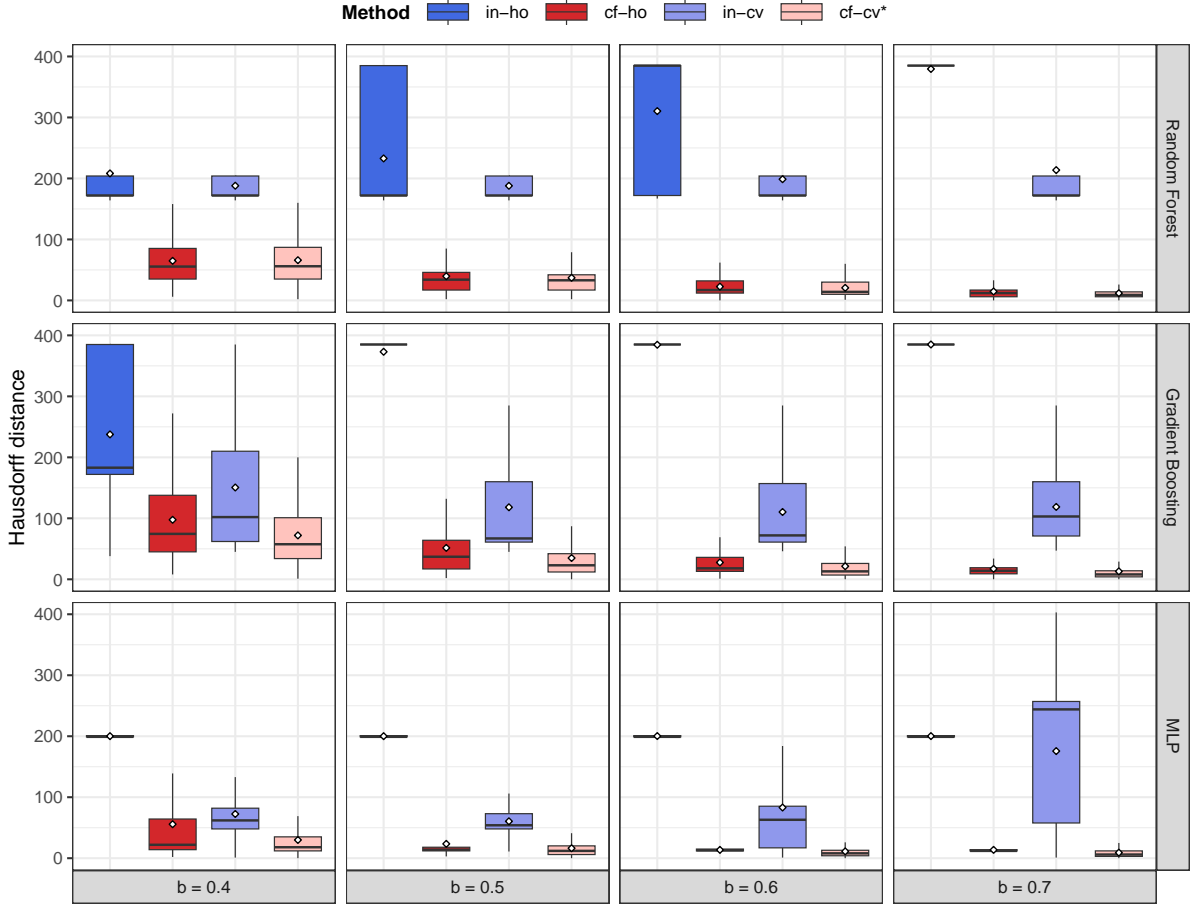


Figure 5: Boxplot of empirical Hausdorff distances for various in-sample and cross-fitting methods in nonparametric changepoint models.

We generate independent samples $z_i \in \mathbb{R}^p, i \in [n]$, with $(n, p) = (1000, 20)$. We set $K^* = 3$ changepoints at locations $\{\tau_k\}_{k=1}^3 = \{350, 500, 880\}$. For $i \in (350, 500] \cup (880, 1000]$, $z_i \sim \mathcal{N}(0, \mathbf{I}_p)$, with \mathbf{I}_p being the identity matrix. For $i \in (0, 350]$, $z_i \sim \mathcal{N}(0, \Sigma)$, where Σ has entries $\Sigma_{ij} = b^{|i-j|}$, reflecting correlation shifts. For $i \in (500, 880]$, $z_i \sim \mathcal{N}(b\mathbf{1}_5, \mathbf{I}_p)$, where b introduces mean shifts. The shift parameter b varies over $\{0.4, 0.5, 0.6, 0.7\}$ to reflect different levels of change signal strength.

Figure 5 illustrates the boxplot of empirical Hausdorff distances for various in-sample and out-of-sample detection approaches, utilizing flexible, modern classifiers. It is clear that in-sample methods often fall short of achieving the desired detection accuracy, largely attributed to the intrinsic overfitting biases that stem from sophisticated model fitting procedures.

Additionally, the detection accuracy does not improve when the change signal level increases. In contrast, the cross-fitting methods demonstrate superior performance in terms of detection accuracy, effectively leveraging the high predictive capabilities of these modern classifiers.

4.3 Array CGH data

This section applies the proposed method to a real dataset—array comparative genomic hybridization (CGH) data—aimed at detecting DNA sequence copy number variations in individuals with bladder tumors. The dataset, accessible from the R package `ecp` (Matteson and James, 2014), includes log intensity ratios of fluorescent DNA segments from $d = 43$ individuals, measured across 2215 loci.

We split the data into two halves: $n = 1108$ odd-indexed observations for changepoint detection, and 1107 even-indexed observations (referred to as test data) for assessing the reliability of the detection outcomes.

In the detection stage, we implement both in-sample and out-of-sample evaluations—**in-cv** and **cf-cv***, integrated with the random forest-based model fitting procedure as described in Section 4.2. Each approach optimizes the total loss with $K \in \{30, 38\}$ ¹.

To assess the reliability of each detected changepoint $\hat{\tau}_j$ for $j \in [K]$ by both **in-cv** and **cf-cv***, we perform a sequence of local two-sample nonparametric tests comparing the test data within the intervals $(\frac{(\hat{\tau}_{j-1} + \hat{\tau}_j)}{2}, \hat{\tau}_j]$ and $(\hat{\tau}_j, \frac{(\hat{\tau}_j + \hat{\tau}_{j+1})}{2}]$. These tests are adjusted using Bonferroni corrections at significance level $\alpha \in \{0.10, 0.05, 0.01\}$, observing the independence among them. We implement the two-sample kernel test proposed by Gretton et al. (2012), using a Gaussian kernel with bandwidth d . A rejection of this test implies that the detected changepoint is “likely” a true positive; otherwise, it may be considered as a false positive.

Table 2 details the number of “false positives” (FPs) and “true positives” (TPs) detected

¹Here, 38 is determined using a hold-out strategy for **in-cv** by further splitting n observations into two parts; one half implements **in-cv** with a sequence of candidate numbers of changepoints and generates a sequence of estimated changepoint models, while the other half calculates the prediction errors associated with each model to select the optimal number of changepoints that minimizes the prediction error. Similarly, 30 is selected for **cf-cv***. It appears that **in-cv** tends to report more changepoints, potentially due to overfitting.

by each of the **in-cv** and **cf-cv*** approaches, with $K \in \{30, 38\}$, alongside the (asymmetric) Hausdorff distance between the sets of TPs detected by both methods:

$$\left\{ \max_{j \in [K]} \min_{k \in [K]} |\widehat{\tau}_{\text{in},k} - \widehat{\tau}_{\text{cf},j}|, \max_{k \in [K]} \min_{j \in [K]} |\widehat{\tau}_{\text{in},k} - \widehat{\tau}_{\text{cf},j}| \right\},$$

which measures the closest proximity of true positive detections between the two methods. These results demonstrate that **cf-cv*** effectively identifies more reliable changepoints with fewer false positives compared to **in-cv**. Moreover, for every TP detected by **in-cv**, **cf-cv*** tends to identify a corresponding TP nearby, as indicated by a smaller value of $\max_{k \in [K]} \min_{j \in [K]} |\widehat{\tau}_{\text{in},k} - \widehat{\tau}_{\text{cf},j}|$. Conversely, **in-cv** sometimes fails to detect a TP identified by **cf-cv***, as reflected by a larger value of $\max_{j \in [K]} \min_{k \in [K]} |\widehat{\tau}_{\text{in},k} - \widehat{\tau}_{\text{cf},j}|$.

Table 2: Number of FPs and TPs detected by the **in-cv** and **cf-cv*** approaches, for array CGH data.

		$\alpha = 0.1$		$\alpha = 0.05$		$\alpha = 0.01$	
		in-cv	cf-cv*	in-cv	cf-cv*	in-cv	cf-cv*
$K = 30$	FP	4	0	4	0	6	1
	TP	26	30	26	30	24	29
	Hausdorff distance	{22, 9}		{22, 9}		{29, 9}	
$K = 38$	FP	12	5	14	5	16	9
	TP	26	33	24	33	22	29
	Hausdorff distance	{20, 6}		{20, 8}		{27, 17}	

5 Concluding remarks

This paper highlights the necessity and benefits of utilizing out-of-sample and cross-fitting evaluations for changepoint detection within the loss minimization framework. It demonstrates how traditional in-sample evaluations can introduce significant overfitting biases, particularly in high-dimensional or nonparametric settings, thus misaligning with the

oracle minimization target. Our approach broadens the potential to integrate flexible, modern predictive algorithms, enhancing changepoint detection capabilities for complex data while ensuring effectiveness, reliability, and reproducibility.

In practice, changepoint search algorithms typically require the specification of the number of changepoints (or the penalty value within the total loss function). Advancing research to develop methods that enable a data-driven selection of the number of changepoints (Zou et al., 2020; Pein and Shah, 2025), seamlessly integrated within the proposed cross-fitting scheme, is imperative. Additionally, it is promising to expand the current loss minimization-based detection framework to include discrepancy-based changepoint detection (Wang and Samworth, 2018; Dette et al., 2022; Cho and Owens, 2024), which entails local comparisons between two, potentially high-dimensional, parameter estimators. While the present method prioritizes consistent changepoint estimation, expanding these techniques to quantify uncertainty in changepoint detection and to enhance post-detection inference is an essential direction for future research; see Chen et al. (2023), Jewell et al. (2022), and Fryzlewicz (2024).

References

- Arlot, S., Celisse, A. and Harchaoui, Z. (2019) A kernel multiple change-point algorithm via model selection. *J. Mach. Learn. Res.*, **20**, (162):1–56.
- Aue, A. and Lee, T. C. M. (2011) On image segmentation using information theoretic criteria. *Ann. Statist.*, **39**, 2912–2935.
- Auger, I. E. and Lawrence, C. E. (1989) Algorithms for the optimal identification of segment neighborhoods. *Bull. Math. Biol.*, **51**, 39–54.
- Bai, J. and Perron, P. (1998) Estimating and testing linear models with multiple structural changes. *Econometrica*, **66**, 47–78.
- Bai, P., Safikhani, A. and Michailidis, G. (2023) Multiple change point detection in reduced rank high dimensional vector autoregressive models. *J. Amer. Statist. Assoc.*, **118**, 2776–2792.
- Bartlett, P. L., Long, P. M., Lugosi, G. and Tsigler, A. (2020) Benign overfitting in linear regression. *Proc. Natl. Acad. Sci. USA*, **117**, 30063–30070.
- Belkin, M., Hsu, D., Ma, S. and Mandal, S. (2019) Reconciling modern machine-learning practice and the classical bias-variance trade-off. *Proc. Natl. Acad. Sci. USA*, **116**, 15849–15854.
- Braun, J. V., Braun, R. K. and Müller, H.-G. (2000) Multiple changepoint fitting via quasilikelihood, with application to DNA sequence segmentation. *Biometrika*, **87**, 301–314.

- Chen, H., Ren, H., Yao, F. and Zou, C. (2023) Data-driven selection of the number of change-points via error rate control. *J. Amer. Statist. Assoc.*, **118**, 1415–1428.
- Chernozhukov, V., Chetverikov, D., Demirer, M., Duflo, E., Hansen, C., Newey, W. and Robins, J. (2018) Double/debiased machine learning for treatment and structural parameters. *Econom. J.*, **21**, C1–C68.
- Chetverikov, D., Liao, Z. and Chernozhukov, V. (2021) On cross-validated Lasso in high dimensions. *Ann. Statist.*, **49**, 1300–1317.
- Cho, H. and Owens, D. (2024) High-dimensional data segmentation in regression settings permitting temporal dependence and non-Gaussianity. *Electron. J. Stat.*, **18**, 2620–2664.
- Csörgő, M. and Horváth, L. (1997) *Limit theorems in change-point analysis*. John Wiley & Sons.
- Dette, H., Pan, G. and Yang, Q. (2022) Estimating a change point in a sequence of very high-dimensional covariance matrices. *J. Amer. Statist. Assoc.*, **117**, 444–454.
- Eichinger, B. and Kirch, C. (2018) A MOSUM procedure for the estimation of multiple random change points. *Bernoulli*, **24**, 526–564.
- Fan, J., Guo, S. and Hao, N. (2012) Variance estimation using refitted cross-validation in ultrahigh dimensional regression. *J. R. Stat. Soc. Ser. B. Stat. Methodol.*, **74**, 37–65.
- Fan, J. and Lv, J. (2008) Sure independence screening for ultrahigh dimensional feature space. *J. R. Stat. Soc. Ser. B. Stat. Methodol.*, **70**, 849–911.
- Fryzlewicz, P. (2014) Wild binary segmentation for multiple change-point detection. *Ann. Statist.*, **42**, 2243–2281.
- (2024) Narrowest significance pursuit: inference for multiple change-points in linear models. *J. Amer. Statist. Assoc.*, **119**, 1633–1646.
- Garreau, D. and Arlot, S. (2018) Consistent change-point detection with kernels. *Electron. J. Stat.*, **12**, 4440–4486.
- Gretton, A., Borgwardt, K. M., Rasch, M. J., Schölkopf, B. and Smola, A. (2012) A kernel two-sample test. *J. Mach. Learn. Res.*, **13**, 723–773.
- Hao, N., Niu, Y. S. and Zhang, H. (2013) Multiple change-point detection via a screening and ranking algorithm. *Statist. Sinica*, **23**, 1553–1572.
- Harchaoui, Z. and Lévy-Leduc, C. (2010) Multiple change-point estimation with a total variation penalty. *J. Amer. Statist. Assoc.*, **105**, 1480–1493.
- Hastie, T., Montanari, A., Rosset, S. and Tibshirani, R. J. (2022) Surprises in high-dimensional ridgeless least squares interpolation. *Ann. Statist.*, **50**, 949–986.
- Jackson, B., Scargle, J. D., Barnes, D., Arabhi, S., Alt, A., Gioumoussis, P., Gwin, E., Sangtrakulcharoen, P., Tan, L. and Tsai, T. T. (2005) An algorithm for optimal partitioning of data on an interval. *IEEE Signal Proc. Lett.*, **12**, 105–108.
- Jewell, S., Fearnhead, P. and Witten, D. (2022) Testing for a change in mean after changepoint detection. *J. R. Stat. Soc. Ser. B. Stat. Methodol.*, **84**, 1082–1104.
- Kaul, A., Jandhyala, V. K. and Fotopoulos, S. B. (2019) An efficient two step algorithm for high dimensional change point regression models without grid search. *J. Mach. Learn. Res.*, **20**, (111):1–40.

- Killick, R., Fearnhead, P. and Eckley, I. A. (2012) Optimal detection of changepoints with a linear computational cost. *J. Amer. Statist. Assoc.*, **107**, 1590–1598.
- Kovács, S., Bühlmann, P., Li, H. and Munk, A. (2023) Seeded binary segmentation: a general methodology for fast and optimal changepoint detection. *Biometrika*, **110**, 249–256.
- Kovács, S., Li, H., Haubner, L., Munk, A. and Bühlmann, P. (2020) Optimistic search: Change point estimation for large-scale data via adaptive logarithmic queries. *arXiv preprint*, arXiv:2010.10194.
- Lee, S., Liao, Y., Seo, M. H. and Shin, Y. (2018) Oracle estimation of a change point in high-dimensional quantile regression. *J. Amer. Statist. Assoc.*, **113**, 1184–1194.
- Lee, S., Seo, M. H. and Shin, Y. (2016) The lasso for high dimensional regression with a possible change point. *J. R. Stat. Soc. Ser. B. Stat. Methodol.*, **78**, 193–210.
- Leonardi, F. and Bühlmann, P. (2016) Computationally efficient change point detection for high-dimensional regression. *arXiv preprint*, arXiv:1601.03704.
- Liu, B., Zhang, X. and Liu, Y. (2021) Simultaneous change point inference and structure recovery for high dimensional Gaussian graphical models. *J. Mach. Learn. Res.*, **22**, (274):1–62.
- Londschien, M., Bühlmann, P. and Kovács, S. (2023) Random forests for change point detection. *J. Mach. Learn. Res.*, **24**, (216):1–45.
- Londschien, M., Kovács, S. and Bühlmann, P. (2021) Change-point detection for graphical models in the presence of missing values. *J. Comput. Graph. Statist.*, **30**, 768–779.
- Matteson, D. S. and James, N. A. (2014) A nonparametric approach for multiple change point analysis of multivariate data. *J. Amer. Statist. Assoc.*, **109**, 334–345.
- Pein, F. and Shah, R. D. (2025) Cross-validation for change-point regression: Pitfalls and solutions. *Bernoulli*, **31**, 388–411.
- Qian, C., Wang, G. and Zou, C. (2023) Reliever: Relieving the burden of costly model fits for changepoint detection. *arXiv preprint arXiv:2307.01150*.
- Rinaldo, A., Wang, D., Wen, Q., Willett, R. and Yu, Y. (2021) Localizing changes in high-dimensional regression models. In *Proceedings of The 24th International Conference on Artificial Intelligence and Statistics*, vol. 130, 2089–2097. PMLR.
- Shi, L., Wang, G. and Zou, C. (2024) Low-rank matrix estimation in the presence of change-points. *J. Mach. Learn. Res.*, **25**, (220):1–71.
- Truong, C., Oudre, L. and Vayatis, N. (2020) Selective review of offline change point detection methods. *Signal Processing*, **167**, 107299.
- Vershynin, R. (2018) *High-dimensional probability*. Cambridge University Press, Cambridge.
- Wang, D., Zhao, Z., Lin, K. Z. and Willett, R. (2021) Statistically and computationally efficient change point localization in regression settings. *J. Mach. Learn. Res.*, **22**, (248):1–46.
- Wang, T. and Samworth, R. J. (2018) High dimensional change point estimation via sparse projection. *J. R. Stat. Soc. Ser. B. Stat. Methodol.*, **80**, 57–83.
- Wang, X., Liu, B., Zhang, X. and Liu, Y. (2024) Efficient Multiple Change Point Detection and Localization For High-Dimensional Quantile Regression with Heteroscedasticity. *J. Amer. Statist. Assoc.*, To appear.

- Williamson, B. D., Gilbert, P. B., Simon, N. R. and Carone, M. (2023) A general framework for inference on algorithm-agnostic variable importance. *J. Amer. Statist. Assoc.*, **118**, 1645–1658.
- Xu, H., Wang, D., Zhao, Z. and Yu, Y. (2024) Change-point inference in high-dimensional regression models under temporal dependence. *Ann. Statist.*, **52**, 999–1026.
- Yao, Y.-C. (1988) Estimating the number of change-points via Schwarz’ criterion. *Statist. Probab. Lett.*, **6**, 181–189.
- Zhang, C., Bengio, S., Hardt, M., Recht, B. and Vinyals, O. (2021) Understanding deep learning (still) requires rethinking generalization. *Commun. ACM*, **64**, 107–115.
- Zhang, Y. and Bradic, J. (2022) High-dimensional semi-supervised learning: in search of optimal inference of the mean. *Biometrika*, **109**, 387–403.
- Zou, C., Wang, G. and Li, R. (2020) Consistent selection of the number of change-points via sample-splitting. *Ann. Statist.*, **48**, 413–439.
- Zou, C., Yin, G., Feng, L. and Wang, Z. (2014) Nonparametric maximum likelihood approach to multiple change-point problems. *Ann. Statist.*, **42**, 970–1002.
- Zrnic, T. and Candès, E. J. (2024) Cross-prediction-powered inference. *Proc. Natl. Acad. Sci. USA*, **121**, (15):1–12.

Supplementary Material for

“Changepoint Detection in Complex Models: Cross-Fitting Is Needed”

The supplementary material includes all theoretical proofs and additional numerical details.

S.1 Proof of Lemma 1

We introduce additional notations that will be used in the proof. For a candidate changepoint $\tau \in [n]$ and a set of benchmark changepoints $\mathcal{T} = \{0 < \tau_1 < \dots < \tau_K < \tau_{K+1} < n\}$, denote $\mathcal{K}_+(\tau, \mathcal{T}) \triangleq \min_k \{k : \tau_k > \tau\}$ and $\mathcal{K}_-(\tau, \mathcal{T}) \triangleq \max_k \{k : \tau_k < \tau\}$. For simplicity, denote $k_{\tau,+}^* = \mathcal{K}_+(\tau, \mathcal{T}^*)$, $\widehat{k}_{\tau,+} = \mathcal{K}_+(\tau, \widehat{\mathcal{T}})$, $k_{\tau,-}^* = \mathcal{K}_-(\tau, \mathcal{T}^*)$ and $\widehat{k}_{\tau,-} = \mathcal{K}_-(\tau, \widehat{\mathcal{T}})$. Recall that the change signal $\Delta_k = \{\bar{\ell}_{\tau_k^*}(f_{k+1}^*) - \bar{\ell}_{\tau_k^*}(f_k^*)\} \vee \{\bar{\ell}_{\tau_k^*+1}(f_k^*) - \bar{\ell}_{\tau_k^*+1}(f_{k+1}^*)\}$. We introduce a related notion to measure the signal of change for any index set $I \subseteq (0, n]$. Specifically, $\Delta_I = |I|^{-1} \{\bar{\mathcal{L}}_I(f_I^\circ) - \bar{\mathcal{L}}_I^*\}$, where $\bar{\mathcal{L}}_I^* = \mathbb{E}[\mathcal{L}_I^*]$ with $\mathcal{L}_I^* = \sum_{i \in I} \ell(z_i, f_i^\circ)$. Denote $d_k = \widetilde{C} d_{\text{acc},n} \Delta_k^{-1}$, and define the set of heterogeneous intervals $\mathcal{I}^{\text{heter}} = \{(s, e] : \exists h \in [K^*], \min(\tau_h^* - s, e - \tau_h^*) > d_h\}$.

Assume that $\mathcal{H} = \{(\widehat{\tau}_a, \widehat{\tau}_{a+1}] : (\widehat{\tau}_a, \widehat{\tau}_{a+1}] \in \mathcal{I}^{\text{heter}}\} \neq \emptyset$, i.e., $\exists h \in [K^*]$ such that $\widehat{\mathcal{T}} \cap [\tau_h^* - d_h, \tau_h^* + d_h] = \emptyset$. For such h and a , without loss of generality, assume that $\tau_h^* - \widehat{\tau}_a > d_h$. It can be observed that $(\tau_h^* - d_h, \tau_h^* + d_h) \subset (\widehat{\tau}_a, \widehat{\tau}_{a+1}]$ and $(\widehat{\tau}_a, \widehat{\tau}_{a+1}] \notin \mathcal{I}^{\text{homo}}$. By Condition 3(c), we have $\Delta_{(\widehat{\tau}_a, \widehat{\tau}_{a+1}]}(\widehat{\tau}_{a+1} - \widehat{\tau}_a) \geq 2d_h \Delta_{(\tau_h^* - d_h, \tau_h^* + d_h)} \geq C_\Delta^{-1} d_h \Delta_h = C_\Delta^{-1} \widetilde{C} d_{\text{acc},n}$.

Definition S.1 (Separability of a point). For a candidate changepoint τ , let $u = k_{\tau,-}^*$ and $v = k_{\tau,+}^*$. This τ is separable from the left (or right) if $\tau - \tau_u^* > d_u \vee d_m$ ($\tau_v^* - \tau > d_v \vee d_m$, respectively). Otherwise, τ is inseparable from the left (right, respectively).

Definition S.2 (Separability of an interval). $\mathcal{H} = \mathcal{H}_1 \cup \mathcal{H}_2 \cup \mathcal{H}_3 \cup \mathcal{H}_4$, where

\mathcal{H}_1 composes of all separable intervals $(\tau_l, \tau_r]$ (τ_l is separable from the right and τ_r is separable from the left);

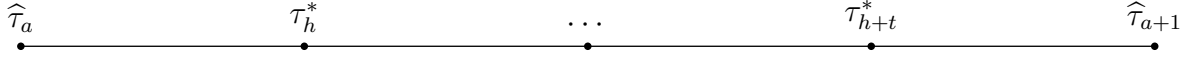
\mathcal{H}_2 composes of all left-separable intervals $(\tau_l, \tau_r]$ (τ_l is separable from the right and τ_r is inseparable from the left);

\mathcal{H}_3 composes of all right-separable intervals $(\tau_l, \tau_r]$ (τ_l is inseparable from the right and τ_r is separable from the left).

\mathcal{H}_4 composes of all inseparable intervals $(\tau_l, \tau_r]$ (τ_l is inseparable from the right and τ_r is inseparable from the left).

We will show that $\mathcal{H} = \emptyset$.

Case 1: $\mathcal{H}_1 = \emptyset$

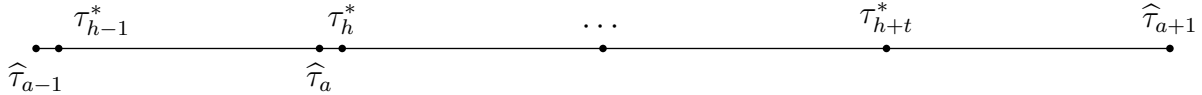


For $(\hat{\tau}_a, \hat{\tau}_{a+1}] \in \mathcal{H}_1$, let $h = k_{\hat{\tau}_a, +}^*$, $\mathcal{T}_a = \{\tau_h^*, \dots, \tau_{h+t}^*\} = \mathcal{T}^* \cap (\hat{\tau}_a, \hat{\tau}_{a+1})$ and $\tilde{\mathcal{T}} = \hat{\mathcal{T}} \cup \mathcal{T}_a$. Since $\gamma = C_\gamma d_{\text{acc}, n}$,

$$\begin{aligned} \mathcal{L}(\hat{\mathcal{T}}) - \mathcal{L}(\tilde{\mathcal{T}}) &= \mathcal{L}_{(\hat{\tau}_a, \hat{\tau}_{a+1}]} - \left[\mathcal{L}_{(\hat{\tau}_a, \tau_h^*]} + \mathcal{L}_{(\tau_{h+t}^*, \hat{\tau}_{a+1}]} + \sum_{j=h}^{h+t-1} \mathcal{L}_{(\tau_j^*, \tau_{j+1}^*]} + (t+1)\gamma \right] \\ &> (1 - C_{1.2}) \Delta_{(\hat{\tau}_a, \hat{\tau}_{a+1}]}^2 (\hat{\tau}_{a+1} - \hat{\tau}_a) - C_{1.1} d_{\text{acc}, n} - (t+2) C_{1.1} d_{\text{acc}, n} - (t+1)\gamma \\ &\geq \left[(1 - C_{1.2})(t+1) C_\Delta^{-1} \tilde{C} - (t+3) C_{1.1} - (t+1) C_\gamma \right] d_{\text{acc}, n} > 0, \end{aligned}$$

provided that $\tilde{C} \geq (1 - C_{1.2})^{-1} C_\Delta (3C_{1.1} + C_\gamma)$. The first inequality is from the fact that $(\hat{\tau}_a, \hat{\tau}_{a+1}] \in \mathcal{I}^{\text{heter}}$ and other intervals are belong to $\mathcal{I}^{\text{homo}}$. Therefore, $\mathcal{H}_1 = \emptyset$.

Case 2: $\mathcal{H}_2 = \mathcal{H}_3 = \emptyset$



Without loss of generality, by the symmetry of \mathcal{H}_2 and \mathcal{H}_3 , we only show that $\mathcal{H}_3 = \emptyset$. If this claim does not hold, one can choose $(\hat{\tau}_a, \hat{\tau}_{a+1}] \in \mathcal{H}_3$ to be the leftmost one. Hence $\hat{\tau}_a$ must

be separable from the left by Condition 3. Since $\mathcal{H}_1 = \emptyset$ and $(\widehat{\tau}_a, \widehat{\tau}_{a+1}]$ is the leftmost interval in \mathcal{H}_3 , one obtains $(\widehat{\tau}_{a-1}, \widehat{\tau}_a] \notin \mathcal{H}$. Denote $h = k_{\widehat{\tau}_a, +}^*$ and $\mathcal{T}_a = \mathcal{T}^* \cap (\widehat{\tau}_a + d_m, \widehat{\tau}_{a+1} - d_m) = \{\tau_{h+1}^*, \dots, \tau_{h+t}^*\}$ ($t = 0$ if $\mathcal{T}_a = \emptyset$). Let $\widetilde{\mathcal{T}} = (\widehat{\mathcal{T}} \setminus \widehat{\tau}_a) \cup \tau_h^* \cup \mathcal{T}_a = (\widehat{\mathcal{T}} \setminus \widehat{\tau}_a) \cup \{\tau_j^*\}_{j=h}^{h+t}$.

$$\begin{aligned} \mathcal{L}(\widehat{\mathcal{T}}) - \mathcal{L}(\widetilde{\mathcal{T}}) &= \mathcal{L}_{(\widehat{\tau}_a, \widehat{\tau}_{a+1}]} + \left(\mathcal{L}_{(\widehat{\tau}_{a-1}, \widehat{\tau}_a]} - \mathcal{L}_{(\widehat{\tau}_{a-1}, \tau_h^*]} \right) - \left[\sum_{j=h}^{h+t-1} \mathcal{L}_{(\tau_j^*, \tau_{j+1}^*]} + \mathcal{L}_{(\tau_{h+t}^*, \widehat{\tau}_{a+1}]} + t\gamma \right] \\ &> (1 - C_{1.2})\Delta_{(\widehat{\tau}_a, \widehat{\tau}_{a+1}]}^2(\widehat{\tau}_{a+1} - \widehat{\tau}_a) - [(t+1)C_{1.1} + tC_\gamma]d_{\text{acc},n} \\ &\quad + \left(\mathcal{L}_{(\widehat{\tau}_a, \tau_h^*]}^* + \mathcal{L}_{(\widehat{\tau}_{a-1}, \widehat{\tau}_a]} - \mathcal{L}_{(\widehat{\tau}_{a-1}, \tau_h^*]} \right). \end{aligned} \quad (\text{S.1})$$

Since $(\widehat{\tau}_{a-1}, \widehat{\tau}_a] \notin \mathcal{H}$ and $0 < \tau_h^* - \widehat{\tau}_a < d_m$, one must obtain that either $(\widehat{\tau}_{a-1}, \widehat{\tau}_a) \cap \mathcal{T}^* = \emptyset$ or $0 < \tau_{h-1}^* - \widehat{\tau}_{a-1} < d_{h-1} = \widetilde{C}\Delta_{h-1}^{-1}d_{\text{acc},n}$.

For the first scenario, under $\mathbb{G}^{\text{nhomo}}$, $\mathcal{L}_{(\widehat{\tau}_{a-1}, \tau_h^*]} - \mathcal{L}_{(\widehat{\tau}_{a-1}, \tau_h^*]}^* \leq C_{1.1}d_{\text{acc},n}$. Under $\mathbb{G}^{-\text{nhomo}}$, $\mathcal{L}_{(\widehat{\tau}_{a-1}, \widehat{\tau}_a]} - \mathcal{L}_{(\widehat{\tau}_{a-1}, \widehat{\tau}_a]}^* > -C_{1.1}d_{\text{acc},n}$ because $\overline{\mathcal{L}}_{(\widehat{\tau}_{a-1}, \widehat{\tau}_a]}(f_{(\widehat{\tau}_{a-1}, \widehat{\tau}_a]}) - \overline{\mathcal{L}}_{(\widehat{\tau}_{a-1}, \widehat{\tau}_a]}^* = 0$. In summary, under $\mathbb{G}^{\text{nhomo}} \cap \mathbb{G}^{-\text{nhomo}}$,

$$\mathcal{L}_{(\widehat{\tau}_a, \tau_h^*]}^* + \mathcal{L}_{(\widehat{\tau}_{a-1}, \widehat{\tau}_a]} - \mathcal{L}_{(\widehat{\tau}_{a-1}, \tau_h^*]} > -2C_{1.1}d_{\text{acc},n}.$$

Therefore,

$$\begin{aligned} \mathcal{L}(\widehat{\mathcal{T}}) - \mathcal{L}(\widetilde{\mathcal{T}}) &> (1 - C_{1.2})\Delta_{(\widehat{\tau}_a, \widehat{\tau}_{a+1}]}(\widehat{\tau}_{a+1} - \widehat{\tau}_a) - [(t+3)C_{1.1} + tC_\gamma]d_{\text{acc},n} \\ &\geq \{(1 - C_{1.2})(t \vee 1)C_\Delta^{-1}\widetilde{C} - (t+4)C_{1.1} - tC_\gamma\}d_{\text{acc},n} > 0, \end{aligned}$$

provided that $\widetilde{C} \geq (1 - C_{1.2})^{-1}C_\Delta(5C_{1.1} + C_\gamma)$.

For the second scenario, let $I_1 = (\widehat{\tau}_{a-1}, \widehat{\tau}_a]$ and $I_2 = (\widehat{\tau}_{a-1}, \tau_h^*]$. We will derive the upper bound of $\Delta_{I_2}|I_2|$ and $\Delta_{I_1}|I_1|$, and show that the difference $\Delta_{I_2}|I_2| - \Delta_{I_1}|I_1|$ is small. Since $I_1 \subset I_2$, we have $\Delta_{I_2}|I_2| - \Delta_{I_1}|I_1| \geq 0$. Since $0 < \tau_{h-1}^* - \widehat{\tau}_{a-1} < d_{h-1} = \widetilde{C}\Delta_{h-1}^{-1}d_{\text{acc},n}$, we have $\Delta_{I_1}|I_1| \leq \Delta_{I_2}|I_2| \leq \overline{\mathcal{L}}_{I_2}(f_h^*) - \overline{\mathcal{L}}_{I_2}^* = \overline{\mathcal{L}}_{(\widehat{\tau}_{a-1}, \tau_{h-1}^*]}(f_h^*) - \overline{\mathcal{L}}_{(\widehat{\tau}_{a-1}, \tau_{h-1}^*]}^*(f_{h-1}^*) \leq d_{h-1}\Delta_{h-1} = \widetilde{C}d_{\text{acc},n}$. Denote $d_1 = \tau_{h-1}^* - \widehat{\tau}_{a-1}$, $d_2 = \widehat{\tau}_a - \tau_{h-1}^*$ and $d_3 = \tau_h^* - \widehat{\tau}_a$. By the definition of $\Delta_{(\cdot)}$, we have $\Delta_{I_1}|I_1| \geq \frac{d_2}{d_2+d_3}\Delta_{I_2}|I_2|$. Hence, $0 \leq \Delta_{I_2}|I_2| - \Delta_{I_1}|I_1| \leq \Delta_{I_2}|I_2|\{1 - d_2/(d_2 + d_3)\} = \Delta_{I_2}|I_2|d_3/(d_2 + d_3) \leq \widetilde{C}d_{\text{acc},n}d_3/(d_2 + d_3) \leq (C_m/C_{\text{snr}})\widetilde{C}d_{\text{acc},n}$. Denote $C_{m,1} = (C_m/C_{\text{snr}})$. Because C_{snr} is sufficiently large, $0 < C_{m,1} \ll 1$ and we can set

$$0 < C_{m,1} < (4C_\Delta)^{-1}\{1 - (1 + 4C_\Delta)C_{1.2}\}. \quad (\text{S.2})$$

By the fact that $\Delta_{I_1}|I_1| \leq \Delta_{I_2}|I_2| \leq \tilde{C}d_{\text{acc},n}$, under $\mathbb{G}^{-\text{nhomo}}$, $\mathcal{L}_{I_1} - \bar{\mathcal{L}}_{I_1}^* - \Delta_{I_1}|I_1| > -\{(C_{1.2}\tilde{C}) \vee C_{1.1}\}d_{\text{acc},n} \geq -(C_{1.2}\tilde{C} + C_{1.1})d_{\text{acc},n}$. Since $I_2 \in \mathcal{I}^{\text{nhomo}}$, we have $\mathcal{L}_{I_2} - \mathcal{L}_{I_2}^* - \Delta_{I_2}|I_2| \leq C_{1.1}d_{\text{acc},n}$ under $\mathbb{G}^{\text{nhomo}}$. In summary, under $\mathbb{G}^{\text{nhomo}} \cap \mathbb{G}^{-\text{nhomo}}$,

$$\mathcal{L}_{(\hat{\tau}_a, \tau_h^*)}^* + \mathcal{L}_{(\hat{\tau}_{a-1}, \hat{\tau}_a]} - \mathcal{L}_{(\hat{\tau}_{a-1}, \tau_h^*)} > -\{2C_{1.1} + (C_{1.2} + C_{m,1})\tilde{C}\}d_{\text{acc},n}. \quad (\text{S.3})$$

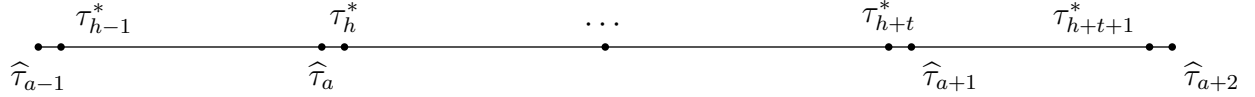
Combining Eq. (S.3) with Eq. (S.1), under $\mathbb{G}^{\text{nhomo}} \cap \mathbb{G}^{-\text{nhomo}}$,

$$\begin{aligned} \mathcal{L}(\widehat{\mathcal{T}}) - \mathcal{L}(\widetilde{\mathcal{T}}) &> (1 - C_{1.2})\Delta_{(\hat{\tau}_a, \hat{\tau}_{a+1})}^2(\hat{\tau}_{a+1} - \hat{\tau}_a) - [(t+3)C_{1.1} + tC_\gamma + (C_{1.2} + C_{m,1})\tilde{C}]d_{\text{acc},n} \\ &\geq \{(1 - C_{1.2})(t \vee 1)C_\Delta^{-1}\tilde{C} - (C_{1.2} + C_{m,1})\tilde{C} - (t+4)C_{1.1} - tC_\gamma\}d_{\text{acc},n} > 0, \end{aligned}$$

provided that $\tilde{C} \geq \{1 - (1 + C_\Delta)C_{1.2} - C_\Delta C_{m,1}\}^{-1}C_\Delta(5C_{1.1} + C_\gamma)$.

Hence, $\mathcal{H}_2 \cup \mathcal{H}_3 = \emptyset$.

Case 3: $\mathcal{H}_4 = \emptyset$



Similar to Case 2, let $(\hat{\tau}_a, \hat{\tau}_{a+1}] \in \mathcal{H}_4$, and thus $\hat{\tau}_a$ is separable from the left and $\hat{\tau}_{a+1}$ is separable from the right. By the fact that $\mathcal{H}_1 \cup \mathcal{H}_2 \cup \mathcal{H}_3 = \emptyset$, we obtain $(\hat{\tau}_{a-1}, \hat{\tau}_a] \notin \mathcal{H}$ and $(\hat{\tau}_{a+1}, \hat{\tau}_{a+2}] \notin \mathcal{H}$. Let $h = k_{\hat{\tau}_a, +}^*$ and $h+t = k_{\hat{\tau}_{a+1}, -}^*$. Denote $\mathcal{T}_a = \{\tau_h^*, \dots, \tau_{h+t}^*\}$ and $\widetilde{\mathcal{T}} = (\widehat{\mathcal{T}} \setminus \{\hat{\tau}_a, \hat{\tau}_{a+1}\}) \cup \mathcal{T}_a$. We have

$$\begin{aligned} \mathcal{L}(\widehat{\mathcal{T}}) - \mathcal{L}(\widetilde{\mathcal{T}}) &= \mathcal{L}_{(\hat{\tau}_a, \hat{\tau}_{a+1})} + [\mathcal{L}_{(\hat{\tau}_{a-1}, \hat{\tau}_a]} + \mathcal{L}_{(\hat{\tau}_{a+1}, \hat{\tau}_{a+2})} - \mathcal{L}_{(\hat{\tau}_{a-1}, \tau_h^*)} - \mathcal{L}_{(\tau_{h+t}^*, \hat{\tau}_{a+2})}] \\ &\quad - \sum_{j=h}^{h+t-1} \mathcal{L}_{(\tau_j^*, \tau_{j+1}^*)} - (t-1)\gamma \\ &> (1 - C_{1.2})\Delta_{(\hat{\tau}_a, \hat{\tau}_{a+1})}(\hat{\tau}_{a+1} - \hat{\tau}_a) - \{(t+1)C_{1.1} + (t-1)C_\gamma\}d_{\text{acc},n} \\ &\quad + [\mathcal{L}_{(\hat{\tau}_a, \tau_h^*) \cup (\tau_{h+1}^*, \hat{\tau}_{a+1})}^* + \mathcal{L}_{(\hat{\tau}_{a-1}, \hat{\tau}_a]} + \mathcal{L}_{(\hat{\tau}_{a+1}, \hat{\tau}_{a+2})} - \mathcal{L}_{(\hat{\tau}_{a-1}, \tau_h^*)} - \mathcal{L}_{(\tau_{h+t}^*, \hat{\tau}_{a+2})}]. \end{aligned}$$

Following arguments similar to those used in Case 2 (Eq. (S.3)), we have

$$\begin{aligned} &\mathcal{L}_{(\hat{\tau}_a, \tau_h^*) \cup (\tau_{h+1}^*, \hat{\tau}_{a+1})}^* + \mathcal{L}_{(\hat{\tau}_{a-1}, \hat{\tau}_a]} + \mathcal{L}_{(\hat{\tau}_{a+1}, \hat{\tau}_{a+2})} - \mathcal{L}_{(\hat{\tau}_{a-1}, \tau_h^*)} - \mathcal{L}_{(\tau_{h+t}^*, \hat{\tau}_{a+2})} \\ &> -2\{2C_{1.1} + (C_{1.2} + C_{m,1})\tilde{C}\}d_{\text{acc},n}. \end{aligned}$$

Hence,

$$\begin{aligned}
& \mathcal{L}(\widehat{\mathcal{T}}) - \mathcal{L}(\widetilde{\mathcal{T}}) \\
& > (1 - C_{1.2})\Delta_{(\widehat{\tau}_a, \widehat{\tau}_{a+1})}^2(\widehat{\tau}_{a+1} - \widehat{\tau}_a) - [(t+5)C_{1.1} + (t-1)C_\gamma + 2(C_{1.2} + C_{m,1})\widetilde{C}]d_{\text{acc},n} \\
& \geq \left\{ (1 - C_{1.2})C_\Delta^{-1}[(t-1) \vee 1]\widetilde{C} - 2(C_{1.2} + C_{m,1})\widetilde{C} - (t+5)C_{1.1} - (t-1)C_\gamma \right\} d_{\text{acc},n} \geq 0,
\end{aligned}$$

provided that $\widetilde{C} \geq \{1 - (1 + 2C_\Delta)C_{1.2} - 2C_\Delta C_{m,1}\}^{-1}C_\Delta(7C_{1.1} + C_\gamma + 2C_{m,1})$.

In summary, we obtain $\mathcal{H} = \emptyset$ provided that $\widetilde{C} \geq \{1 - (1 + C_\Delta)C_{1.2} - 2C_\Delta C_{m,1}\}^{-1}C_\Delta(7C_{1.1} + C_\gamma + 2C_{m,1})$. Hence $\max_{1 \leq j \leq K^*} \min_{1 \leq k \leq \widehat{K}} \Delta_j^2 |\tau_j^* - \widehat{\tau}_k| \leq \widetilde{C}d_{\text{acc},n}$. It also implies that $\widehat{K} \geq K^*$.

It remains to show that $\widehat{K} \leq K^*$. Otherwise, assume that $\widehat{K} > K^*$. Then there must be $j \in [0, K^*]$ and $k \in [1, \widehat{K}]$ such that $\widehat{\tau}_{k-1} \in [\tau_j^* - d_j, \tau_j^* + d_j]$ and $\widehat{\tau}_{k+t} \in [\tau_{j+1}^* - d_{j+1}, \tau_{j+1}^* + d_{j+1}]$ for some $t \geq 1$. Without loss of generality, assume that $t = 1$. Similar to the decomposition of \mathcal{H} , we can divide this event into four groups:

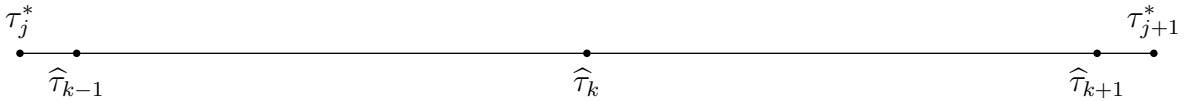
$$\mathcal{G}_1 : \tau_j^* \leq \widehat{\tau}_{k-1} < \widehat{\tau}_k < \widehat{\tau}_{k+1} \leq \tau_{j+1}^*.$$

$$\mathcal{G}_2 : \tau_j^* - d_j \leq \widehat{\tau}_{k-1} < \tau_j^* \text{ and } \tau_j^* \leq \widehat{\tau}_k < \widehat{\tau}_{k+1} \leq \tau_{j+1}^*.$$

$$\mathcal{G}_3 : \tau_j^* \leq \widehat{\tau}_{k-1} < \widehat{\tau}_k \leq \tau_{j+1}^* \text{ and } \tau_{j+1}^* < \widehat{\tau}_{k+1} \leq \tau_{j+1}^* + d_{j+1}.$$

$$\mathcal{G}_4 : \tau_j^* - d_j \leq \widehat{\tau}_{k-1} < \tau_j^* \leq \widehat{\tau}_k \leq \tau_{j+1}^* < \widehat{\tau}_{k+1} \leq \tau_{j+1}^* + d_{j+1}$$

Case 1: $\mathcal{G}_1 = \emptyset$



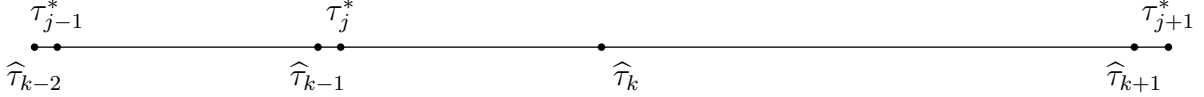
Let $\widetilde{\mathcal{T}} = \widehat{\mathcal{T}} \setminus \{\widehat{\tau}_k\}$. We have

$$\begin{aligned}
\mathcal{L}(\widetilde{\mathcal{T}}) - \mathcal{L}(\widehat{\mathcal{T}}) &= \mathcal{L}_{(\widehat{\tau}_{k-1}, \widehat{\tau}_{k+1})} - \mathcal{L}_{(\widehat{\tau}_{k-1}, \widehat{\tau}_k)} - \mathcal{L}_{(\widehat{\tau}_k, \widehat{\tau}_{k+1})} - \gamma \\
&< (3C_{1.1} - C_\gamma)d_{\text{acc},n} \leq 0,
\end{aligned}$$

provided that $C_\gamma \geq 3C_{1.1}$.

Case 2: $\mathcal{G}_2 \cup \mathcal{G}_3 = \emptyset$

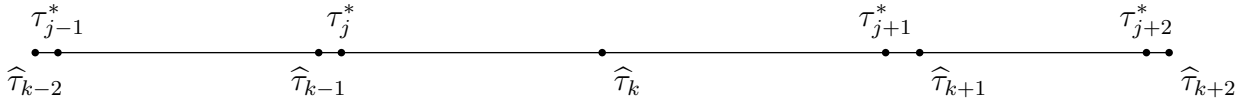
We will show that $\mathcal{G}_2 = \emptyset$ because the proof for $\mathcal{G}_3 = \emptyset$ is similar by the symmetry. Assume that $\{j, k\}$ is the leftmost case that satisfies \mathcal{G}_2 . It implies that $\widehat{\tau}_{k-2} \in [\tau_{j-1}^* - d_{j-1}, \tau_{j-1}^* + d_{j-1}]$. Otherwise assume $\widehat{\tau}_{k-2} > \tau_{j-1}^* + d_{j-1}$. Since $\max_{1 \leq j \leq K^*} \min_{1 \leq k \leq \widehat{K}} \Delta_j^2 |\tau_j^* - \widehat{\tau}_k| \leq \widetilde{C} d_{\text{acc}, n} / 2$, there must be $\widehat{\tau}_{k-h} \in [\tau_{j-1}^* - d_{j-1}, \tau_{j-1}^* + d_{j-1}]$ for some $h > 2$. It contradicts with $\mathcal{G}_1 = \emptyset$ and the choice of k . Let $\widetilde{\mathcal{T}} = \{\tau_j^*\} \cup \widehat{\mathcal{T}} \setminus \{\widehat{\tau}_{k-1}, \widehat{\tau}_k\}$.



$$\begin{aligned}
\mathcal{L}(\widetilde{\mathcal{T}}) - \mathcal{L}(\widehat{\mathcal{T}}) &= \mathcal{L}(\widehat{\tau}_{k-2}, \tau_j^*) + \mathcal{L}(\tau_j^*, \widehat{\tau}_{k+1}) - \left[\sum_{t=k-2}^k \mathcal{L}(\widehat{\tau}_t, \widehat{\tau}_{t+1}) + \gamma \right] \\
&= [\mathcal{L}(\widehat{\tau}_{k-2}, \tau_j^*) - \mathcal{L}(\widehat{\tau}_{k-2}, \widehat{\tau}_{k-1})] + \mathcal{L}(\tau_j^*, \widehat{\tau}_{k+1}) - \left[\sum_{t=k-1}^k \mathcal{L}(\widehat{\tau}_t, \widehat{\tau}_{t+1}) + \gamma \right] \\
&< \left[\mathcal{L}(\widehat{\tau}_{k-2}, \tau_j^*) - \mathcal{L}(\widehat{\tau}_{k-2}, \widehat{\tau}_{k-1}) - \mathcal{L}^*(\widehat{\tau}_{k-1}, \tau_j^*) \right] + (3C_{1.1} - C_\gamma) d_{\text{acc}, n} \\
&\leq \{5C_{1.1} + (C_{1.2} + C_{m,1})\widetilde{C} - C_\gamma\} d_{\text{acc}, n} \leq 0,
\end{aligned}$$

provided that $C_\gamma \geq 5C_{1.1} + (C_{1.2} + C_{m,1})\widetilde{C}$. The first inequality is from the facts that $(\tau_j^*, \widehat{\tau}_{k+1}) \in \mathcal{I}^{\text{homo}}$, $(\widehat{\tau}_k, \widehat{\tau}_{k+1})$ contains no changepoints and for $I = (\widehat{\tau}_{k-1}, \widehat{\tau}_k) \notin \mathcal{I}^{\text{homo}}$, $\mathcal{L}_I - \mathcal{L}_I^* > \Delta_I |I| - (C_{1.2} \Delta_I |I|) \vee (C_{1.1} d_{\text{acc}, n}) > -C_{1.1} d_{\text{acc}, n}$ because $0 < C_{1.2} < 1$. The second inequality is from Eq. (S.3).

Case 3: $\mathcal{G}_4 = \emptyset$



Now $\mathcal{G}_1 \cup \mathcal{G}_2 \cup \mathcal{G}_3 = \emptyset$. Assume that $\{\widehat{\tau}_{k-1}, \widehat{\tau}_k, \widehat{\tau}_{k+1}\}$ satisfies \mathcal{G}_4 . Similar to Case 2, we have $\widehat{\tau}_{k-2} \in [\tau_{j-1}^* - d_{j-1}, \tau_{j-1}^* + d_{j-1}]$ and $\widehat{\tau}_{k+2} \in [\tau_{j+1}^* - d_{j+1}, \tau_{j+1}^* + d_{j+1}]$. Following arguments

similar to those used in Case 2, with $\tilde{\mathcal{T}} = \{\tau_j^*, \tau_{j+1}^*\} \cup \hat{\mathcal{T}} \setminus \{\hat{\tau}_{k-1}, \hat{\tau}_k, \hat{\tau}_{k+1}\}$, we obtain

$$\begin{aligned}
\mathcal{L}(\tilde{\mathcal{T}}) - \mathcal{L}(\hat{\mathcal{T}}) &= \mathcal{L}_{(\hat{\tau}_{k-2}, \tau_j^*)} + \mathcal{L}_{(\tau_j^*, \tau_{j+1}^*)} + \mathcal{L}_{(\tau_{j+1}^*, \hat{\tau}_{k+2})} - \left[\sum_{t=k-2}^{k+1} \mathcal{L}_{(\hat{\tau}_t, \hat{\tau}_{t+1})} + \gamma \right] \\
&= [\mathcal{L}_{(\hat{\tau}_{k-2}, \tau_j^*)} - \mathcal{L}_{(\hat{\tau}_{k-2}, \hat{\tau}_{k-1})} + \mathcal{L}_{(\tau_{j+1}^*, \hat{\tau}_{k+2})} - \mathcal{L}_{(\hat{\tau}_{k+1}, \hat{\tau}_{k+2})}] \\
&\quad + \mathcal{L}_{(\tau_j^*, \tau_{j+1}^*)} - \left[\sum_{t=k-1}^k \mathcal{L}_{(\hat{\tau}_t, \hat{\tau}_{t+1})} + \gamma \right] \\
&< \left[\mathcal{L}_{(\hat{\tau}_{k-2}, \tau_j^*)} - \mathcal{L}_{(\hat{\tau}_{k-2}, \hat{\tau}_{k-1})} + \mathcal{L}_{(\tau_{j+1}^*, \hat{\tau}_{k+2})} - \mathcal{L}_{(\hat{\tau}_{k+1}, \hat{\tau}_{k+2})} - \mathcal{L}_{(\hat{\tau}_{k-1}, \tau_j^*) \cup (\tau_{j+1}^*, \hat{\tau}_{k+1})} \right] \\
&\quad + (3C_{1.1} - C_\gamma)d_{\text{acc},n} \leq \{7C_{1.1} + 2(C_{1.2} + C_{m,1})\tilde{C} - C_\gamma\}d_{\text{acc},n} \leq 0,
\end{aligned}$$

provided $C_\gamma \geq 7C_{1.1} + 2(C_{1.2} + C_{m,1})\tilde{C}$.

Combining all things regarding \mathcal{H} and \mathcal{G} together, we can determine the two constants \tilde{C} and C_γ by solving the following inequalities,

$$\begin{cases} C_\gamma \geq 7C_{1.1} + 2(C_{1.2} + C_{m,1})\tilde{C}, \\ \tilde{C} \geq \{1 - (1 + 2C_\Delta)C_{1.2} - 2C_\Delta C_{m,1}\}^{-1}C_\Delta(7C_{1.1} + C_\gamma + 2C_{m,1}). \end{cases}$$

By setting C_{snr} sufficiently large, $C_{m,1} = C_m/C_{\text{snr}}$ is sufficiently small and Eq. (S.2) holds.

Let $C_\gamma = 7C_{1.1} + 2(C_{1.2} + C_{m,1})\tilde{C}$, one obtains the following inequality,

$$\{1 - (1 + 2C_\Delta)C_{1.2} - 2C_\Delta C_{m,1}\}\tilde{C} \geq C_\Delta\{14C_{1.1} + 2C_{m,1} + 2(C_{1.2} + C_{m,1})\tilde{C}\}.$$

It is equivalent to,

$$\tilde{C} \geq \{1 - (1 + 4C_\Delta)C_{1.2} - 4C_\Delta C_{m,1}\}^{-1}C_\Delta(14C_{1.1} + 2C_{m,1}). \quad (\text{S.4})$$

We can choose $\tilde{C} = \{1 - (1 + 4C_\Delta)C_{1.2} - 4C_\Delta C_{m,1}\}^{-1}C_\Delta(14C_{1.1} + 2C_{m,1})$ and $C_\gamma = 7C_{1.1} + 2(C_{1.2} + C_{m,1})\tilde{C}$. With the choices of \tilde{C} and C_γ , we have $\hat{\mathcal{T}} = \tilde{\mathcal{T}}$ and

$$\hat{K} = K^*; \quad \max_{1 \leq k \leq K^*} \min_{1 \leq j \leq \hat{K}} \Delta_k |\tau_k^* - \hat{\tau}_j| \leq \tilde{C}d_{\text{acc},n}.$$

S.2 Proof of Theorem 1

It suffices to check that the events $\mathbb{G}^{\text{nhomo}}$ and $\mathbb{G}^{-\text{nhomo}}$ in Lemma 1 hold with high probability. The key lies in deriving concentration bounds for the empirical losses based on the following Bernstein's inequality.

Lemma S.1 (Bernstein's inequality). *For independent random variables $\{X_i\}_{i=1}$ with bounded Ψ_1 -norm,*

$$\mathbb{P}\left(\left|\sum_i X_i\right| \geq t\right) \leq 2 \exp\left[-c \min\left(\frac{t^2}{\sum_i \|X_i\|_{\Psi_1}^2}, \frac{t}{\max_i \|X_i\|_{\Psi_1}}\right)\right].$$

Recall $J_m = \{i \in [n] : (i-1) \bmod M = m-1\}$ and denote $J_{m,I} := J_m \cap I$, for $m \in [M]$. For any index set I , denote $\Delta_{I,f} = |I|^{-1}\{\bar{\mathcal{L}}_I(f) - \bar{\mathcal{L}}_I^*\}$, which extends the notion Δ_I via $\Delta_{I,f^\circ} = \Delta_I$.

First, consider $\mathbb{G}^{\text{nhomo}}$. For $I \in \mathcal{I}^{\text{nhomo}}$, we have $\Delta_I|I| \leq 2\tilde{C}d_{\text{acc},n}$. Because $J_m \cap I \subset I$, it also holds that $\Delta_{I \cap J_m}|I \cap J_m| \leq \Delta_{I \cap J_m, f_I^\circ}|I \cap J_m| \leq 2\tilde{C}d_{\text{acc},n}$. By the assumption that $\bar{\mathcal{L}}_{I \cap J_m}(\hat{f}_{I \setminus J_m}) - \bar{\mathcal{L}}_{I \cap J_m}(f_I^\circ) \lesssim d_{\text{acc},n}$, we have $\Delta_{I \cap J_m, \hat{f}_{I \setminus J_m}}|I \cap J_m| \lesssim \tilde{C}d_{\text{acc},n}$. Denote $s_i = \ell(z_i; \hat{f}_{I \setminus J_m}) - \ell(z_i; f_i^\circ) - \bar{\ell}_i(\hat{f}_{I \setminus J_m}) + \bar{\ell}_i(f_i^\circ)$. By conditions that $\sup_k \Delta_k \lesssim d_{\text{acc},n}/\log n$, $\bar{\mathcal{L}}_{I \cap J_m}(\hat{f}_{I \setminus J_m}) - \bar{\mathcal{L}}_{I \cap J_m}(f_I^\circ) \lesssim d_{\text{acc},n}$ and $|I| \geq C_m d_{\text{acc},n} \gtrsim \log n$, we have $|\bar{\ell}_i(\hat{f}_{I \setminus J_m}) - \bar{\ell}_i(f_i^\circ)| \lesssim d_{\text{acc},n}/\log n$. Therefore, $\max_{i \in I \cap J_m} \|s_i\|_{\Psi_1} \lesssim d_{\text{acc},n}/\log n$ and $\sum_{i \in I \cap J_m} \|s_i\|_{\Psi_1}^2 \lesssim (d_{\text{acc},n}/\log n)\Delta_{I \cap J_m, \hat{f}_{I \setminus J_m}}|I \cap J_m| = (d_{\text{acc},n}/\log n)\{\Delta_{I \cap J_m, f_I^\circ}|I \cap J_m| + \bar{\mathcal{L}}_{I \cap J_m}(\hat{f}_{I \setminus J_m}) - \bar{\mathcal{L}}_{I \cap J_m}(f_I^\circ)\} \lesssim \tilde{C}d_{\text{acc},n}^2/\log n$. By Bernstein's inequality, with probability at least $1 - \exp(-C \log n)$,

$$\sum_{i \in I \cap J_m} s_i \lesssim \tilde{C}^{\frac{1}{2}} d_{\text{acc},n}.$$

By the assumption that $\bar{\mathcal{L}}_{I \cap J_m}(\hat{f}_{I \setminus J_m}) - \bar{\mathcal{L}}_{I \cap J_m}(f_I^\circ) \lesssim d_{\text{acc},n}$, and taking the summation over $m \in [M]$ and the union bound over $I \in \mathcal{I}^{\text{nhomo}}$, we have with probability at least $1 - \exp(-C \log n)$, uniformly for all $I \in \mathcal{I}^{\text{nhomo}}$,

$$\xi_I(\mathcal{L}_I) = \sum_{m \in [M]} \{\mathcal{L}(z_{I \cap J_m}; \hat{f}_{I \setminus J_m})\} - \sum_{i \in I} \ell(z_i; f_i^\circ) - \Delta_I^2|I| \lesssim \tilde{C}^{\frac{1}{2}} d_{\text{acc},n}.$$

The lower bound holds similarly.

Next, consider $\mathbb{G}^{-\text{nhomo}}$. For $I \notin \mathcal{I}^{\text{nhomo}}$ such that $\Delta_I|I| \lesssim \tilde{C}d_{\text{acc},n}$, similarly we have $\Delta_{I \cap J_m}|I \cap J_m| \lesssim \tilde{C}d_{\text{acc},n}$ and $\sum_{i \in I \cap J_m} \|s_i\|_{\Psi_1}^2 \lesssim \Delta_{I \cap J_m, \hat{f}_{I \setminus J_m}}|I \cap J_m|d_{\text{acc},n}/\log n \lesssim \tilde{C}d_{\text{acc},n}^2/\log n$ and $\max_{i \in I \cap J_m} \|s_i\|_{\Psi_1} \lesssim d_{\text{acc},n}/\log n$. Therefore, with probability at least $1 - \exp(-C \log n)$,

$$\sum_{i \in I \cap J_m} s_i \gtrsim -\tilde{C}^{\frac{1}{2}} d_{\text{acc},n},$$

which ensures that

$$\xi_I(\mathcal{L}_I) \gtrsim -\tilde{C}^{\frac{1}{2}} d_{\text{acc},n}.$$

For $I = (s, e] \notin \mathcal{I}^{\text{nhomo}}$ such that $\Delta_I |I| \gtrsim \tilde{C} d_{\text{acc},n}$, by the order-preserved splitting scheme, we claim $\Delta_{I \cap J_m} |I \cap J_m| \gtrsim \tilde{C} d_{\text{acc},n}$. The reason is that because $\Delta_I |I| \gtrsim \tilde{C} d_{\text{acc},n}$, there must be a changepoint $\tau_k \in I$ such that $\min(\tau_k - s, e - \tau_k) \gtrsim \tilde{C} \Delta_k^{-1} d_{\text{acc},n}$. And since $\Delta_k^{-1} d_{\text{acc},n} \gtrsim \log n$, we have $\min(|(s, \tau_k] \cap J_m|, |(\tau_k, e] \cap J_m|) \gtrsim \tilde{C} \Delta_k^{-1} d_{\text{acc},n}$. Therefore $\Delta_{I \cap J_m} |I \cap J_m| \gtrsim \tilde{C} d_{\text{acc},n}$. It also holds that $(\Delta_{I \cap J_m, f_I^\circ} |I \cap J_m|) \wedge (\Delta_{I \cap J_m, \hat{f}_{I \setminus J_m}} |I \cap J_m|) \geq \Delta_{I \cap J_m} |I \cap J_m| \gtrsim \tilde{C} d_{\text{acc},n}$. By Condition 2, $|\Delta_{I \cap J_m, f_I^\circ} - \Delta_{I \cap J_m, \hat{f}_{I \setminus J_m}}| \times |I \cap J_m| \lesssim d_{\text{acc},n}$.

We now derive the upper bound of $\max_{i \in I \cap J_m} \|s_i\|_{\Psi_1}$. Assume that I contains K_I changepoints, we have $\Delta_{I \cap J_m, \hat{f}_{I \setminus J_m}} |I \cap J_m|, \Delta_I |I| \gtrsim \{\tilde{C} + \max((K_I - 2), 0) C_{\text{snr}}\} d_{\text{acc},n}$. By the assumption that $\sup_k \Delta_k \lesssim d_{\text{acc},n} / \log n$, $\max_{i \in I \cap J_m} \|s_i\|_{\Psi_1} \lesssim \Delta_{I \cap J_m, \hat{f}_{I \setminus J_m}} + K_I d_{\text{acc},n} / \log n \lesssim (C_m^{-1} + \tilde{C}^{-1}) \Delta_{I \cap J_m, \hat{f}_{I \setminus J_m}} |I \cap J_m| / \log n$. Therefore, $\sum_{i \in I \cap J_m} \|s_i\|_{\Psi_1}^2 \lesssim (C_m^{-1} + \tilde{C}^{-1}) \Delta_{I \cap J_m, \hat{f}_{I \setminus J_m}}^2 |I \cap J_m|^2 / \log n$. Define the positive constant

$$C' = (\Delta_{I \cap J_m, \hat{f}_{I \setminus J_m}} |I \cap J_m|)^{-1} \max \left\{ \max_{i \in I \cap J_m} \|s_i\|_{\Psi_1} \log n, \left(\sum_{i \in I \cap J_m} \|s_i\|_{\Psi_1}^2 \log n \right)^{1/2} \right\}.$$

By Bernstein's inequality, with probability at least $1 - \exp(-C \log n)$ with C be some universal constant,

$$\mathcal{L}(z_{I \cap J_m}; \hat{f}_{I \setminus J_m}) - \mathcal{L}_{I \cap J_m}^* - \Delta_{I \cap J_m, \hat{f}_{I \setminus J_m}} |I \cap J_m| \geq -C' (C_m^{-1/2} + \tilde{C}^{-1/2}) \Delta_{I \cap J_m, \hat{f}_{I \setminus J_m}} |I \cap J_m|.$$

By taking the summation over $m \in [M]$, we have with probability at least $1 - \exp(-C \log n)$, uniformly for all I ,

$$\sum_{m \in [M]} \{\mathcal{L}(z_{I \cap J_m}; \hat{f}_{I \setminus J_m})\} - \sum_{i \in I} \ell(z_i; f_i^\circ) - \Delta_I |I| \gtrsim (C_m^{-1/2} + \tilde{C}^{-1/2}) \Delta_I |I|.$$

Overall, we have $\mathbb{P}(\mathbb{G}^{\text{nhomo}} \cap \mathbb{G}^{-\text{nhomo}}) \geq 1 - \exp(-\Omega(\log n))$ with $C_{1.1} = C \tilde{C}^{1/2}$ and $C_{1.2} = C(C_m^{-1/2} + \tilde{C}^{-1/2})$ for some universal constant $C > 0$.

Based on the choices of $C_{1.1}$ and $C_{1.2}$, there is \tilde{C} that only depends on $C_m, C_{\text{snr}}, C_\Delta$ and satisfies Eq. (S.4) in the proof of Lemma 1. With such a \tilde{C} , Theorem 1 holds.

S.3 Proof of Proposition 1

For the squared loss, we have the following result,

$$\begin{aligned}
\xi_I(\mathcal{L}_I) &= \sum_{i \in I} [\{u_i + x_i^\top (f_I^\circ - \widehat{f}_I)\}^2 - \epsilon_i^2] - \mathbb{E}(\|u_I\|^2) + \sigma_\epsilon^2 |I| \\
&= \sum_{i \in I} [u_i^2 - \epsilon_i^2 + 2u_i x_i^\top (f_I^\circ - \widehat{f}_I) + \{x_i (f_I^\circ - \widehat{f}_I)\}^2] - \sum_{i \in I} \|f_i^\circ - f_I^\circ\|_\Sigma^2 \\
&= \sum_{i \in I} [2\epsilon_i x_i^\top (f_i^\circ - f_I^\circ) + \{x_i^\top (f_i^\circ - f_I^\circ)\}^2 - \|f_i^\circ - f_I^\circ\|_\Sigma^2] \\
&\quad - 2u_I^\top X_I (\widehat{f}_I - f_I^\circ) + \|X_I (\widehat{f}_I - f_I^\circ)\|^2.
\end{aligned}$$

By Condition 1', $\max_{i \in I} \|f_i^\circ - f_I^\circ\|_\Sigma^2 \leq C_f s_n$, we have $\text{Var}[\sum_{i \in I} 2\epsilon_i x_i^\top (f_i^\circ - f_I^\circ) + \{x_i^\top (f_i^\circ - f_I^\circ)\}^2 - \|f_i^\circ - f_I^\circ\|_\Sigma^2] \lesssim C_f s_n \sum_{i \in I} \|f_i^\circ - f_I^\circ\|_\Sigma^2$. Therefore, we conclude that

$$\xi_I(\mathcal{L}_I) = O_p\left(\sqrt{\sum_{i \in I} \|f_i^\circ - f_I^\circ\|_\Sigma^2 s_n \log n}\right) - 2u_I^\top X_I (\widehat{f}_I - f_I^\circ) + \|X_I (\widehat{f}_I - f_I^\circ)\|^2.$$

Analyses of bias terms in Proposition 1

Table S1: Terms contributing to the bias for a given homogeneous segment I .

Loss	Model	Cross	Squared
In-sample	$\widehat{f}_I^{\text{lasso}}(\lambda^\circ)$	$O_p(s_n \log p)$	$O_p(s_n \log p)$
In-sample	$\widehat{f}_I^{\text{lasso}}(\widehat{\lambda}_I^{\text{cv}})$	$O_p(\ u_I^\top X_I\ _\infty \cdot \sqrt{ \widehat{S}_I + s_n} \cdot \ \widehat{f}_I - f_I^\circ\ _2)$ $= O_p(\sqrt{ I \log p} \cdot \sqrt{ \widehat{S}_I + s_n} \cdot \sqrt{s_n (\log^2 p) / I }) O_p(s_n \log^2 p)$ $= O_p(\sqrt{(\widehat{S}_I + s_n) s_n \log^3 p})$	
Out-of-sample	$\widehat{f}_{I \setminus J_m}^{\text{lasso}}(\widehat{\lambda}_{I \setminus J_m}^{\text{cv}})$	$O_p(\sqrt{s_n \log^2 p})$	$O_p(s_n \log^2 p)$

Table S1 compares the contributors to bias in both in-sample and out-of-sample loss evaluations, demonstrating how out-of-sample loss evaluations could mitigate the effects of bias on detection precision through these cross terms.

S.4 Proof of Corollary 1

It suffices to demonstrate that Conditions 1–3 are satisfied with $d_{\text{acc},n} = s_n^2 \log p$. Condition 1 and Condition 3(b) are ensured by Condition 1'. Condition 2 is guaranteed by Condition 2'. Condition 3(a) aligns with Condition 3'. Lastly, Condition 3(c) is satisfied with $C_\Delta = 2$ for linear models with squared loss.

S.5 DGP Regarding Ridgeless Regression

We consider $(n, p, K^*) = (500, 1000, 1)$, with $\tau_1^* = 150$. The noises $\{\epsilon_i\}$ are i.i.d. from $\mathcal{N}(0, 1)$, and the covariates x_i are i.i.d. from $\mathcal{N}(\mathbf{0}, \Sigma)$, where the covariance matrix Σ adheres to the benign setting detailed in Bartlett et al. (2020, Theorem 2). Let \mathbf{v}_j denote the eigenvector corresponding to the j -th largest eigenvalue of Σ . We define the coefficients $f_1^* = \sum_{j=1}^5 \mathbf{v}_j / \sqrt{5}$ and $f_2^* = \sum_{j=1}^5 (-1)^j \mathbf{v}_j / \sqrt{5}$.